From the Research Laboratories
В изследователските лаборатории

PHARMACOKINETICS, DRUG-LIKENESS, MEDICINAL PROPERTIES, MOLECULAR DOCKING ANALYSIS OF SUBSTITUTED B-LACTAMS SYNTHEZIED VIA [BMIM][PF6]/]$ET_3NH]^+[HSO_4]^-$ CATALYZED COUPLING REACTION

[1)]Ajay M. Ghatole, [2)]Mahesh K. Gaidhane, [3)]Kushal R. Lanjewar, [1)]Kishor M. Hatzade

[1)]Dhote Bandhu Science College (India)
[2)]Shri Lemdeo Patil Mahavidyalaya (India)
[3)]Mohsin Bhai Zawer College (India)

Abstract. Our examination planned to synthesize the azido β-lactam under reactive ionic liquids for new synthetic organic methodologies. These endeavors may provide more clarity to the analysis in the systems of natural responses utilizing ionic liquid as response media. The Schiff base witnesses quick responses with azido acidic acid in a [bmim] $[PF_6]/[Et_3NH]^+[HSO_4]^-$ dissolvable framework, under mellow and unbiased response conditions to afford the corresponding azido β-lactam in high to quantitative yields. The library of substituted 3-azido-4-phenyl-1-(-phenylthiazol-2-yl) azetidin-2-one (**3a-s**) has screened antibacterial movement against clinically secluded Gram-positive bacteria, for example, *Staphylococcus aureus*, Gram-negative microbes *Escherichia coli* and *Pseudomonas aeruginosa* and for antifungal action against *Candida albicans* strains. Further, the synthesized compound has also assessed by a computational investigation by cooperation with the dynamic site of E150K from MRSA (PDB ID-4BL2). We present the new SwissADME web utensil that gives free access to a pool of quick yet reliable analytical models for physicochemical properties, pharmacokinetics, drug-likeness, and medicinal chemistry. Among them, in-house capable technique, for example, BOILED-Egg, iLOGP, and Bioavailability Radar, are readily available on the web.

Keywords: ionic liquid; azido β-lactam; MRSA; SwissADME; BOILED-egg; bioavailability radar

Introduction

In the nineteenth century, azides and azido-related compounds (Rostovtsev et al., 2002) demonstrate the enormous enthusiasm by researchers, the synthesis and reactivity of multifunctional allylic azides become a territory of dynamic research (Cardillo et al., 2005; Feldman et al., 2005; Mangelinckx et al., 2005). In the combination of natu-

ral product and nitrogen-containing heterocycles, allylic azides are adaptable building blocks with pharmacological significance (Busetto et al., 1975; Rigby et al., 1979). In specific metal complexes, the coordinated azide responds under generally mellow conditions with electron-poor nitriles (Beck & Fehlhammer, 1967; Fehlhammer et al., 1979), and isonitriles (Pino-Gonzalez et al., 2008) deliver metal-nitrogen, and metal-carbon reinforced tetrazoles, individually. Azide acts as an amino securing cluster (Amantini et al., 2002; Larock, 1989; Scriven & Turnbull, 1988) and is impervious to numerous response conditions; however, it can effectively diminish to amines. The researcher puts a great deal of exertion to portray proficient azido reduction techniques Mitchell et al., 2007; Nyffeler et al., 2002), and some of them connected in carbohydrate functionalization (Busetto et al., 1975; Rigby et al., 1979; Silverman & Dolphin, 1976). In Photoaffinity naming system (Schnapp et al., 1993) the perfluorophenyl azides (Fig. 1) has a vital job and is utilized for the marking of DNA binding proteins (Dezhurov et al., 2005; Lavrik et al., 1996; Lee et al., 2002) are in alteration of human ribosome (Demeshkina et al., 2003a; 2003b), functionalization of bifunctional chelating specialists for γ–imaging, radiotherapy (Lin et al., 2016) and for biotin-labeled photoaffinity tests (Han et al., 2006a; 2006b). The azido nucleosides (Fig. 2) are the genomic building blocks, which interface with nucleic acids, enzymes, and proteins (El Akri et al., 2007), which are significant constituents of living cells.

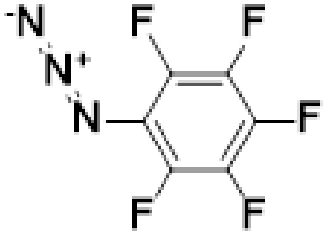

Figure 1. Perfluorophenyl azide

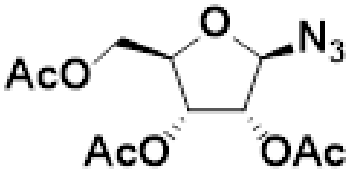

Figure 2. Azido nucleosides

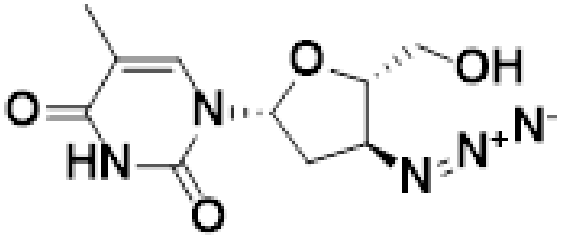

Figure 3. 3-azido-3-deoxythymidine

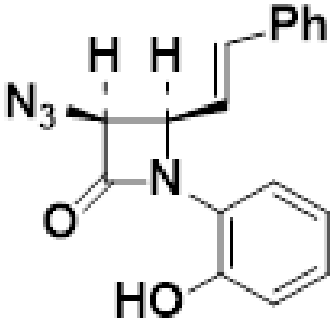

Figure 4. (3S,4R,E)-3-azido-1-(2-hydroxyphenyl)-4-styrylazetidin-2-one

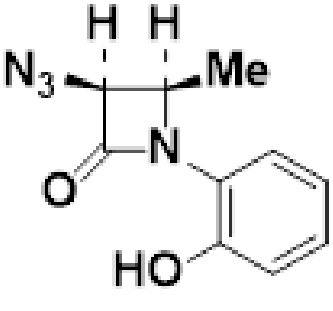

Figure 5. (3S,4R)-3-azido-1-(2-hydroxyphenyl)-4-methylazetidin-2-one

For the treatment of human immunodeficiency infection (HIV) replication, 3-azido-3-deoxythymidine (AZT) (Fig.3) has primarily been authorized medication, and it also shows short half-life in the body and symptoms (Botta et al., 1998). The (3S,4R)-3-azido-1-(2-hydroxyphenyl)-4-((E)- styryl)azetidin-2-one (Fig.4) show feeble antibacterial movement and great anticancer property (Hakimelahi & Sardarian, 1990), while (3S,4R)-3-azido-1-(2-hydroxyphenyl)-4-((E)-methyl) azetidin-2-one (Fig.5) shows none.

In this context, it is to note that Ajay Bose et al. (1992) prepared azido β–lactam (Fig. 6) from azido acetyl chloride.

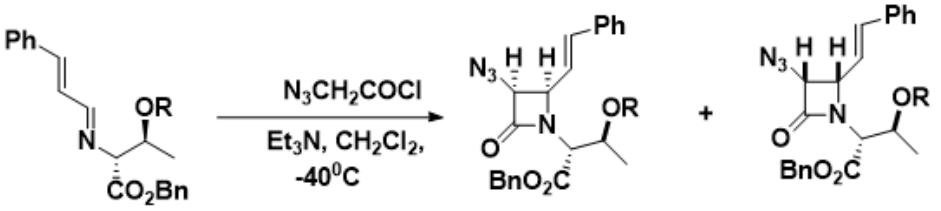

Figure 6. Azido β-lactam

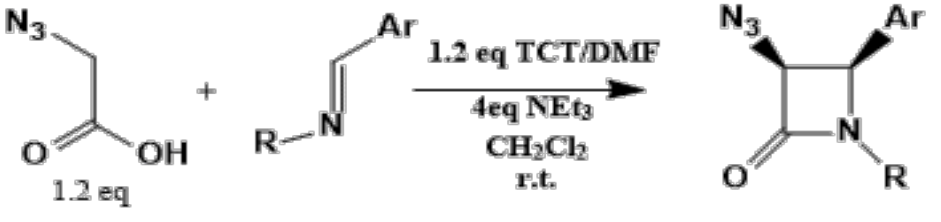

Figure 7. (3S,4R)-3-azido-1-substituted-4-phenylazetidin-2-one

In the support Zarei et al. (2011) prepared azido β–lactam (Fig. 7) by efficient conversion of Schiff base by reaction with 2-azidoacetic acid under room temperature.

Reduced thiazole serves in the investigation of polypeptides as a basic unit in compounds of biological imperative, and 2-amino-thiazole has histamine-like action (Ghatole, Lanjewar, & Gaidhane, Syntheses, Characterization, Antimicrobial activity of Copper (II), Zinc (II) and Cobalt (II) Complexes of the bi-dented substituted 2-((E)-2-((2-chloro-6-ethoxyquinolin-3-yl), 2012). We imagined joining a β-lactam ring and different heterocycles in a solitary atom, despite barely any writing reports giving primary, gentle, and efficient routes towards a combination of substituted 3-azido-4-phenyl-1-(- phenylth-

iazol-2-yl)azetidin-2-one moieties. Generally, a medical clinic tainted by the establishment of a clone of Methicillin-safe Staphylococcus aureus (MRSA), which prompts numerous maladies like skin disease, pneumonia, bacteremia Daum et al., 2002). In some cases, there are mortality and ailment, likewise seen by MRSA contamination, it is a direct result of the obstruction created by the Staphylococcus aureus against treatment (Rossi et al., 2014). The β-lactam antimicrobial like Methicillin, Vancomycin, Teicoplanin, Telavancin, and Ceftaroline utilized for the treatment brought about by the infection of Staphylococcus aureus. The ceftaroline, a recently endorsed medication which restrains penicillin-binding protein (PBP2a) by setting off an allosteric conformational change that prompts the opening of the dynamic site. Presently the second atom of ceftaroline controls the unprotected opened dynamic site. Now the second molecule of ceftaroline inhibits the defenseless opened active site that damages cell-wall, which leads to bacterial death (Fishovitz et al., 2014). In methicillin, Ceftaroline, Penicillin has the β-lactam and thiazole unit in structure. By considering the result of the writing study, we have structured the new molecule of β-lactam with azide functional group to give a productive biomechanical path successfully.

SwissADME is an excellent and exhaustive site kept running by the Swiss foundation of bioinformatics (SIB), which gives bioinformatics administrations and assets to researchers around the world. SIB has more than 65 bioinformatics research gatherings and 800 researchers from the real Swiss schools of advanced education and research institute. SwissADME empowers the appraisal of ADME parameters of medication applicants and small molecules and gives data that permits early hazard evaluation in the drug improvement process. Eminently, swissADME provides a stage to evaluate Lipinski's rule of five (Lipinski et al., 2001) for medication resemblance of oral bioavailability. Drug-likeness is an unpredictable equalization of molecular properties and structural features that decide if an unfamiliar molecule resembles the known drug. These molecular properties incorporate hydrophobicity, electronic dispersion, and hydrogen bonding attributes molecular size and adaptability. SwissADME includes 'BOILEDegg' assessment (Daina & Zoete, 2016) that foresee gastrointestinal captivation (HIA) and efflux/maintenance by P-glycoprotein (Pgp). Also, the blood-brain barrier (BBB) infiltration and Cytochrome P450 (CYP) enzyme substrate-restraint expectation can make.

Besides, there are expanding worries about ecological impacts, which require manufactured control that limit the utilization of hazardous chemicals. Numerous procedures have concocted and examined, particularly by supplanting the customary organic with other non-toxic solvents, for example, water or supercritical carbon dioxide. As of late, ionic liquids have pulled in broad enthusiasm as superb options in contrast to organic solvents, because of their

favorable properties, for example, non-combustibility, no quantifiable vapor pressure, low toxicity, reusability, low-cost and high thermal stability (Gordon, 2001l Sheldon, 2001). Notwithstanding the polar properties of ionic liquids, they are non- coordinating, which maintains a strategic distance from any undesired solvent binding in pre-transition states and henceforth offers incredible points of interest for asymmetric synthesis. Subsequently, ionic liquids considered promising elective solvents for organic reactions. In recent years, these liquids have produced a lot of intrigues (Katritzky et al., 2000; Alkiyama et al., 1999l Wenzel & Jacobsen, 2002). In the present examination, the principle preferred standpoint of the utilization of ionic liquids is that these liquid salts can effectively recuperate on workup. Since the items were genuinely dissolvable in the ionic fluids, they could be effectively isolated by straightforward extraction with ether. The staying ionic liquid was utterly washed with ether and reused.

Result and discussion

Chemistry

The impact of solvent for the amalgamation of substituted 3-azido-4-phenyl-1-(4-phenylthizole-2-yl)azetidin-2-one (**3a-b**) from substituted N-(4-benzylidene)- 4-(4-phenyl)thiazol-2-amine (**2a-b**) and azido acidic acid under the various condition of time and temperature of refluxed dissolvable organized in Table 1. In the present examination, we have synthesized the azido derivatives of **3a-b** in different solvents like DMF, DMSO, CH_3CN, CH_2Cl_2 under the presence of triethylamine in the other investigation we utilized [bmim][PF_6] and [bmim][PF_6]/[Et_3NH]$^+$[HSO_4]$^-$ without triethylamine as a solvent. Bronsted acidic quaternary ammonium sulfate $Et_3NH]^+[HSO_4]^-$ Ghatole et al., 2015) ionic liquid was utilized as an impetus. In the conventional technique, the yield acquired was nearly low and required additional time. Advancement of reaction conditions for all the reactions uncovered that 1–butyl-3-methylimidazolium-hexafluorophosphate i.e. [bmim][PF_6] with [Et_3NH]$^+$[HSO_4]$^-$ was the suitable solvent. In all reactions, the profitability expanded up to 75-80% with the diminished time factor.

From the above test conditions, it saw that azido derivatives development, promptly happened in the [bmim]PF_6/[Et_3NH]$^+$[HSO_4]$^-$ contrasted with different solvents even nevertheless unadulterated [Et_3NH]$^+$[HSO_4]$^-$ and continues in exceptional yields. So, the further synthesis of the **3a-s** carried out under [bmim]PF_6/[Et_3NH]$^+$[HSO_4]$^-$ with **2 a-s** and N_3CH_2COOH in 1:1 ratio. The ether soluble ionic liquid was recovered by removing under vacuum and reuse for the synthesis. The recycling efficiency of ionic liquid found decreased after three cycles: the isolated yields and every single physical constant classified in Table 2.

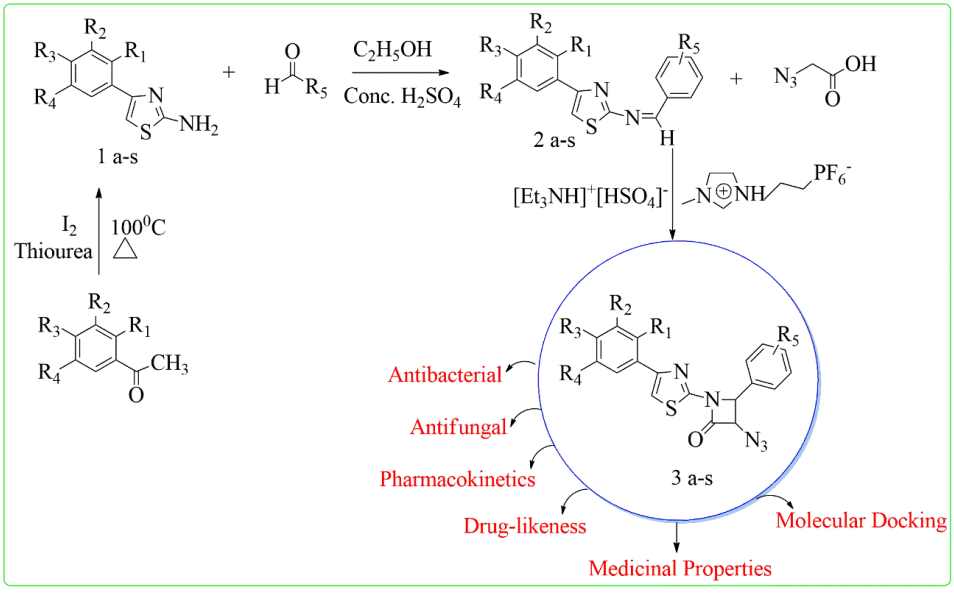

Scheme. - Substituted 3-azido-4-phenyl-1-(-phenylthiazol-2-yl)azetidin-2-one (**3a-s**)

Table 1. Effect of solvent on the synthesis of substituted 3-azido-4-phenyl-1-(4-phenylthizole-2-yl) azetidin-2-one (**3a-b**)

Solvent		Temp (^{0}C)	Time (hr)	Comparisons % yield of 3a-b (Reaction between 2a-b and N_3CH_2COOH in 1:1 ratio)	
				3a	3b
With Et3N	DMF	Reflux	8	67	56
	DMSO	Reflux	8	35	25
	CH_3CN	55-60	5	-	-
	CH_2Cl_2	35-40	6	69	69
Without Et3N	[bmim]PF_6	45-50	4	59	61
	[bmim]PF_6/ $[Et_3NH]$+$[HSO_4]$-	45-50	4	75	80

We endeavored the whole arrangement of reactions with fittingly substituted substrates, and the structures affirmed by CHN, IR, ^{1}H NMR, ^{13}C NMR, Mass fragmentation of the compounds. The expected peak in the IR for (**2a-s**) primary amine

(-NH_2) found inside the area 3350-3570 cm^{-1}, the pinnacle comparing to the methoxy group and C-S-C for **2a** showed up at 2830-2930 cm^{-1} and 771cm^{-1}.

Table 2. Synthesis of substituted 3-azido-4-phenyl-1-(-phenylthiazol-2-yl)azetidin-2-one (**3a-s**)

Sr. No.	Comp.	R_1	R_2	R_3	R_4	R_5	Yield (%)	M. P. (^{0}C)
1	**3a**	H	H	OCH_3	H	4-OCH_3-Ar	75	138
2	**3b**	H	H	CH_3	H	4-OCH_3-Ar	80	205
3	**3c**	H	H	CH_3	H	4-$N(CH_3)_2$-Ar	74	230
4	**3d**	H	H	CH_3	H	3-NO_2-Ar	73	170
5	**3e**	OH	H	H	CH_3	4-OCH_3-Ar	77	170
6	**3f**	OH	I	H	CH_3	4-$N(CH_3)_2$-Ar	69	186
7	**3g**	OH	Br	H	CH_3	4-$N(CH_3)_2$-Ar	74	100
8	**3h**	OH	Br	H	CH_3	4-OCH_3-Ar	78	230
9	**3i**	OH	Br	H	CH_3	4-Cl-Ar	79	94
10	**3j**	OH	Br	H	Cl	4-OCH_3-Ar	85	135
11	**3k**	OH	H	H	Cl	4Cl-Ar	79	110
12	**3l**	OH	Br	H	Cl	3-NO_2-Ar	75	140
13	**3m**	OH	Br	H	Cl	3-Cl-Ar	78	146
14	**3n**	OH	Br	H	Cl	4-$N(CH_3)_2$-Ar	78	>320
15	**3o**	OH	H	H	Cl	Ar	76	94
16	**3p**	OH	NO_2	H	CH_3	Furfural	75	169
17	**3q**	OH	H	H	CH_3	Ar	75	184
18	**3r**	OH	I	H	Cl	4-OCH_3-Ar	79	145
19	**3s**	OH	I	H	Cl	4-$N(CH_3)_2$-Ar	80	132

The ^{1}H NMR 4-(4-methoxyphenyl) thiazol-2-amine **2a** demonstrates a crest as a singlet at δ 3.64 ppm, which corresponds to the amine (-NH_2) group. Moreover, the trademark crest for (**2a-s**) showing up at δ 6.2-7.20 ppm relates to the thiazole ring. However, for the case **2a**, C-H of the thiazole ring shows up at δ 6.96 ppm. One-pot transformation of substituted **2a-s** to the substituted 3-azido-4-phenyl-1-(4-phenylthizole-2-yl)azetidin-2-ones **3a-s** affirmed by the IR spectrum of the compound that

indicated groups at 1670-1720cm^{-1} and 2100-2124cm^{-1} comparing to the β-lactam carbonyl and azido group respectively.

The IR carbonyl frequencies and the ^{13}C NMR compound movements of the carbonyl carbons rely on the ring size and lie in the normal range. For every other compound with four-membered rings, C=O: 165.0– 168.55, C-N_3: 78.01-81.00 showed up. The somewhat extraordinary qualities propose similar stereo structures (barely different conformational circumstances). The ^{1}H NMR range for (**3a-s**) demonstrated that the doublet for C7 and C8 hydrogen of the β-lactam ring in the area δ 5.2-5.8 and δ 6.2-6.8 and the aromatic proton appeared from the region δ 6.64-7.70 ppm. The elemental analysis and molecular ion pinnacles of compounds (**3a-s**) are reliable with the assigned structure.

Pharmacology

The newly synthesized compounds **3a-s** tried for tits in vitro antimicrobial activities against clinical isolates of Gram-positive microbes Staphylococcus aureus and its standard reference (ATCC 6538P), Gram-negative bacteria Pseudomonas aeruginosa, it's a stock reference (ACTT-BAA-427), Escherichia coli (ATCC 8739) and Candida albicans. Along these lines, a progression of azido β-lactams having the thiazole moiety into one molecular framework has been synthesized, which shows slight to direct antibacterial and antifungal action.

Table 3. Zone of inhibition in mm for compounds **3a-s** to reference drugs activity against Gram-negative, gram-positive bacteria and Fungus at concentration 50, 100, 200 µg/ml in DMSO

Entry	Antibacterial activity in µgm/mL (zone of inhibition in mm)									Antifungal activity		
	P. Aeruginous			S. Aureus			E. Coli			C. Albicans		
	200	100	50	200	100	50	200	100	50	200	100	50
3a	10	-	-	16	-	-	8	7	-	10	-	-
3b	10	-	-	17	8	-	10	7	-	10	-	-
3c	8	-	-	8	-	-	8	-	-	8	-	-
3d	10	-	-	12	10	-	9	-	-	10	-	-
3e	-	-	-	15	7	-	6	7	-	28	10	-
3f	6	-	-	15	8	-	6	6	-	25	10	-
3g	8	-	-	16	7	-	9	7	-	12	-	-
3h	8	-	-	12	10	-	9	8	-	21	8	-
3i	8	-	-	17	-	-	6	-	-	-	-	-
3j	8	-	-	13	-	-	5	6	-	12	-	-
3k	8	-	-	15	7	-	8	6	-	11	-	-

3l	8	-	-	15	7	-	10	-	-	26	10	-
3m	8	-	-	12	-	-	7	-	-	11	-	-
3n	6	-	-	12	-	-	7	8	-	20	9	-
3o	8	-	-	11	-	-	6	7	-	26	10	-
3p	6	-	-	13	9	-	8	-	-	10	-	-
3q	-	-	-	11	9	-	-	5	-	13	-	-
3r	6	-	-	8	-	-	8	-	-	8	-	-
3s	-	-	-	10	-	-	-	-	-	9	-	-
SD				30	25	20	20	16	12	-	-	-
SF				-	-	-	-	-	-	30	24	16

SD – Standard Doxycycline, SF – Standard Fluconazole

All compounds **3a-s** demonstrated critical action against Gram-negative Pseudomonas aeruginosa, while **3b** and **3l** showed articulated activity against Escherichia coli. Among every one of the compounds tried against Gram +vie Staphylococcus aureus, just **3b**, **3g**, and **3l** repressed the development of microorganisms altogether while different compounds demonstrated moderate activity (Ghatole et al., 2014).

The antifungal movement results in Table 3 uncovered that mixes compounds **3e**, **3f**, **3h**, **3l**, **3n,** and **3o** had a generally high inhibitory impact on Candida albicans, the remainder of the compound displayed moderate action.

Structure-activity relationships (SAR)

Structure-activity relationships, a great stencil used for tailoring effective lead molecules, were studied. We tested all the synthesized compounds against bacteria and fungus with moderate to high antimicrobial activity.

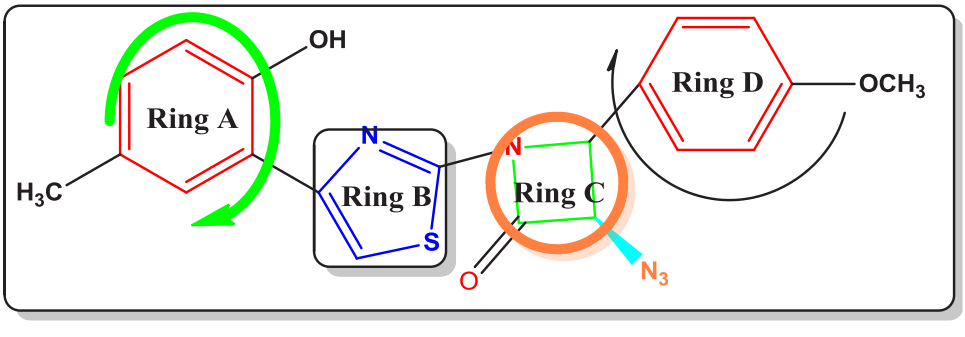

Figure 8. Structure-activity relationships substituted 3-azido-4-phenyl-1-(4-phenylthizole-2-yl)azetidin-2-one (**3a-s**)

Our hybrid molecule may consider as a template scaffold in which one can insert substituents at different positions to enhance the specificity of microorganisms as antibacterial and antifungal activities. Our hybrid molecules possess ring A (Fig. 8) as a substituted aromatic ring in the thiazole skeleton at Ortho, Meta, and Para position. Ring B constitutes the thiazole subunit; ring C is a four-membered cyclic β-lactam ring having the azido group as a substitute at the C8 location, ring D derived from substituting aromatic aldehyde. The compound **3l** displayed maximum antibacterial and antifungal activity at 200 µg/ml due to -OH, -Cl, and -Br substitution on ring A at the ortho, meta, position and $–NO_2$ substitution at 3rd position of ring D. which enhanced the synergistic effects leading to compounds having excellent activity in comparison to other compounds. Either with unsubstituted or substituted aromatic ring D., It is also interesting to note that the compounds **3e**, **3f**, **3h**, **3n** and **3o** exhibit significant antifungal activity, at 200 µg/ml. That reve$_1$ substitution of –OH in all products at ortho position and replacement of –Br and –I at meta position of aromatic ring A and ring B is essential for modulation of the hydrophilic, which may enhance its antifungal activity. The presence of electron-withdrawing group ($-NO_2$) and donating group like $-N(CH_3)_2$, $-OCH_3$ as substituents at the 3rd and 4th positions in rings D may attenuate the antifungal activity. Other compounds exhibited moderate activity against fungi and bacteria due to the presence of $-CH_3$, OH, Cl at ring A, and $–OCH_3$, $-NO_2$, substituents at ring D irrespective of inductive effects.

Molecular modelling

A comparative study done with the known drugs viz. ceftaroline, methicillin, penicillin, doxycycline, fluconazole, teicoplanin, telavancin to the active site of the clinical mutant E150K from MRSA (PDB ID-4BL2) made for better comprehension of their antibiotic action. Docking score depicted in Table 4.

Table 4. Docking score in kcal/mole of the standard antibiotic drug against E150K from MRSA (PDB ID-4BL2) active site of chain A and B

Sr. No.	Ligand	Docking score (Kcal/mole)	
		Chain A	Chain B
1.	Ceftaroline	-5.5	-5.6
2.	Meticillin	-4.2	-4.2
3.	Penicillin	-4.8	-4.3
4.	Doxycycline	-5.3	-4.9
5.	Fluconazole	-4.2	-4.4
6.	Teicoplanin	-6.3	-6.0
7.	Telavancin	4.4	-3.5

The computational test was directed by PyRx programming with eight best conformational positions out of that the best posture esteem detailed in Table 4. Considering the above information without much of a stretch foresee that the standard compounds with active sites of chains A and B. The ceftaroline and teicoplanin had the most significant negative binding energy relations with other approved drugs.

Table 5. Docking score (Kcal/mole) of differently substituted β-lactam analog ligand **3a-s** with PDB ID-4BL2 having site chain A

Sr. No.	Binding affinity in Kcal/mole	Sr. No.	Binding affinity in Kcal/mole
3a	-4.7	**3k**	-4.8
3b	-4.6	**3l**	-4.9
3c	-4.4	**3m**	-4.9
3d	-4.8	**3n**	-4.8
3e	-4.7	**3o**	-4.7
3f	-4.9	**3p**	-4.9
3g	-4.8	**3q**	-4.7
3h	-4.8	**3r**	-4.8
3i	-5.0	**3s**	-4.8
3j	-4.9		

Table 6. Docking score (kcal/mole) of differently substituted β-lactam analog ligand **3a-s** with PDB ID-4BL2 having site chain B

Sr. No.	Binding affinity in Kcal/mole	Sr. No.	Binding affinity in Kcal/mole
3a	-4.5	**3k**	-5.6
3b	-4.6	**3l**	-4.6
3c	-4.6	**3m**	-4.6
3d	-5.2	**3n**	-4.8
3e	-5.5	**3o**	-4.8
3f	-4.6	**3p**	-5.4
3g	-4.4	**3q**	-4.8
3h	-4.8	**3r**	-4.2
3i	-4.8	**3s**	-4.6
3j	-4.6		

From the binding energy score and atomic interaction between the ligand and protein dynamic site of chain A and Chain B, a portion of the perceptions portrayed. The coupling score of ligand **3i** (-5.0Kcal/mole) with chain A had the most note-

worthy negative value, which is comparable to standard drug ceftaroline (-5.5Kcal/mole) yet not exactly teicoplanin (-6.3Kcal/mole). With chain A had **3f**, **3l**, **3j**, **3m**, and **3p** demonstrates the same binding score while **3c** had a rundown score. In chain B interaction **3k** (-5.6Kcal/mol) had a most elevated value which is comparable with the standard teicoplanin (- 6.0Kcal/mole) among the variously blended compound which displayed in Tables 5 and 6.

Comparative interaction study of 3l (-5.0Kcal/mole) vs 3f (-4.9 Kcal/mole) and 3c (-4.4Kcal/mole) LIGPLOT plot with the active site of chain A

The red circles and ovals in each plot show protein residues that are in equal 3D positions to the tailings. Hydrogen bonds appeared green dotted lines, while the spoked bends speak to deposits making non- bonded contacts with the ligand.

HIS311 – Imidazole functional group of histidine demonstrates hydrogen holding with terminal nitrogen of azide functional group of ligands **3i** (3.19A^0) and **3f** (3.25A^0), respectively. The terminal nitrogen of azide in **3i** and nitrogen directly connected azetidine ring in hydrophobic association with HIS311, imidazole ring carbon, and the straightforwardly appended secondary carbon with the imidazole ring, while in the case of **3f** there is no hydrophobic communication.

GLN140 – The iminol form of the glutamine side chain indicates 2.98A^0 and 2.94A^0 hydrogen holding with terminal nitrogen of azide functional group of **3i** and **3c**; with this equivalent nitrogen in **3c** connection and center nitrogen of azide group demonstrates hydrophobic interaction with carbonyl carbon of amide functional group of GLN140. In any case, **3f** just had hydrogen bonding (2.97A^0) of terminal nitrogen of azide bunch with iminol form of the glutamine side chain. With this GLN140 having the carbonyl carbon and oxygen of the amide functional group had hydrophobic communication with two methyls and the nitrogen atom of N-dimethyl benzene substituted ring.

GLY135 – The carboxylic acid group of GLY135 indicates hydrogen bonding, i.e., 2.90A^0 with terminal nitrogen of azide group of **3f** with no other hydrophobic association. While **3i** and **3c** additionally demonstrate hydrogen holding (2.80A^0, 3.24A^0) and hydrophobic association with carbonyl carbon and -NH_2 of GLY135.

VAL302 – The primary amine of VAL302 shows hydrogen bonding with **3i** and **3f** of radius 3.03A^0 and 3.01A^0, respectively, and hydrophobic interaction with the carbonyl oxygen of azetidine ring.

THR300 – THR300 had a carboxylic acid and primary amine group, which is in hydrogen bonding with the nitrogen of thiazole ring (3.06A^0) and hydroxy group (3.03A^0) of a substituted phenyl ring of ligand **3f**. The nitrogen of the thiazole ring and hydroxy group of **3i** had hydrogen bonding with carboxylic acid (3.11A^0), and a primary amine group (2.96A^0) of THR300 expansion to this **3i** demonstrates the number of hydrophobic communications with THR300 which isn't seen with **3f** as portrayed in Fig. 9.

HIS143– We look at the interaction of histidine 143 and 311 with the ligand **3i** and **3f**; both amino acids demonstrate hydrogen holding, yet the bond length is diverse in HIS143. The carboxylic acid group interacts with a hydroxy group of **3i** with hydrogen bond length 3.02A^0, while the same carboxylic acid group of HIS143 shows 3.13A^0 hydrogen bonding with the hydroxy group of **3f**.

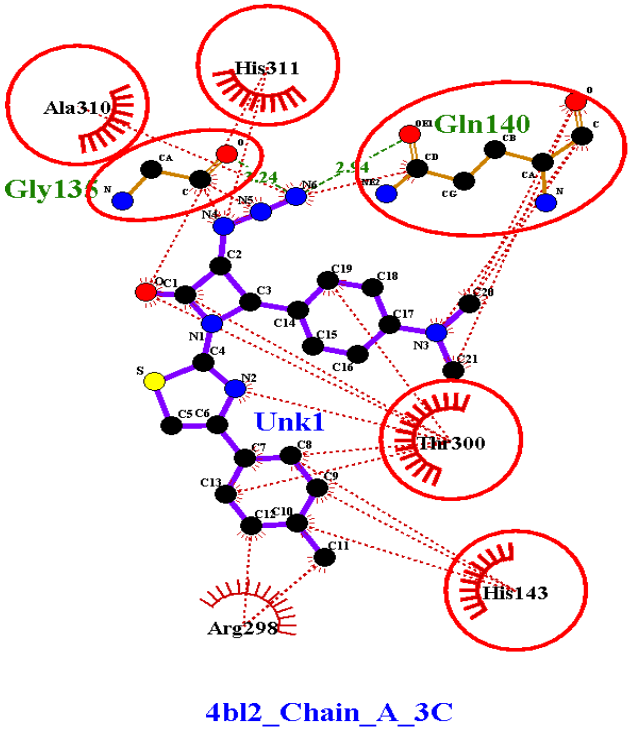

Figure 9. LIGPLOT protein-ligand interaction diagram of chain A (**4bl2_chain_A**) and ligand **3i**, **3f,** and **3c**

Further, HIA143 and **3f** ligand don't demonstrate any hydrophobic interaction, while carbonyl carbon of HIS143 had hydrophobic interaction with bromine and a hydroxy group, which likewise associated in hydrogen bonding. The non-ligand residue, i.e., ALA310, ARG110 in hydrophobic contact with the **3i** and **3f** while in a case on protein-ligand interaction ALA310 and **3c** in hydrophobic connection along with HIS311, THR300, HIS143, and ARG298 that used for hydrogen bonding in protein-ligand (**3f** and **3i**) interaction.

Comparative interaction study of 3k (-5.6 Kcal/mole) vs. list binding energy score 3r (-4.2 Kcal/mole) LIGPLOT plot with the active site of chain B

In the comparative plot of **3k** and **3r** (Fig. 10), there is three amino acids via HIS785, THR942, and VAL944 that are in equivalent 3D positions to the residues. Out of this, only THR942 commonly had hydrogen bonding with the nitrogen of the thiazole ring in **3k** and methoxy oxygen of a substituted benzene ring of **3r**. The **3k** had hydrogen bonding (3.26A^0) with a carboxylic acid group, while **3r** shows hydrogen bonding (3.05A^0) with a hydroxy group of THR942. But only **3k** ligand shows hydrophobic interaction with THR942.

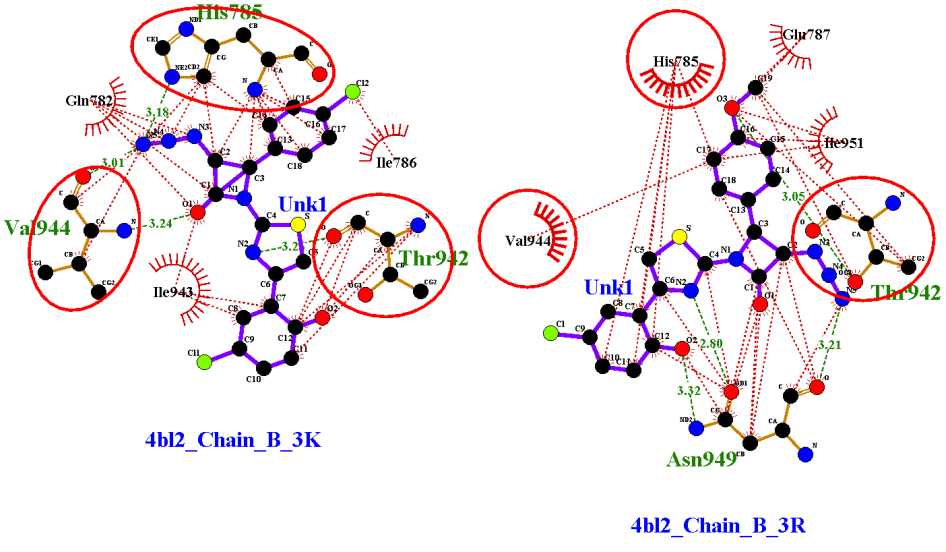

Figure 10. LIGPLOT protein-ligand interaction diagram of chain B (**4bl2_chain_B**) with ligand **3k** and **3r**

HIS785 shows a hydrogen bond (3.18A^0) with terminal nitrogen of azide group and had numerous hydrophobic interactions with the nitrogen of azide, carbon of azetidine, and carbon of chlorophenyl ring of **3k**; in case of **3r** ligand, it had only hydrophobic contact. **3k** shows two hydrogen bonding viz 3.01A^0 and 3.24A^0 with VAL944 while it is absent in **3r**. Another amino acid interaction is GLN782, ILE943, and ILE786 with **3k** and **3r** with the active site of chain B are GLU787 and ILE951.

SwissADME pharmacokinetics, physicochemical, medicinal properties study

The operational highlights of these molecules entered in the SwissADME site (http://swissadme.ch) utilizing the ChemAxon's Marvin JS structure drawing in-

strument. Auxiliary highlights of a pharmacophore impact including bioavailability, transport properties, empathy to proteins, reactivity, poisonous quality, and metabolic steadiness. Incomparable to swissADME is the bioavailability radar (Daina et al., 2017) that gives a graphical preview of the medication similarity parameters of an orally available bioactive drug. The drug resemblance diagram displayed as a hexagon (Figs. 11 and 12) with each of the vertices speaking to a parameter that characterizes a bioavailable drug. The pink region inside the hexagon speaks to the ideal range for every property (lipophilicity: XLOGP3 between −0.7 and +5.0, size: polarity: TPSA (Topological Polar Surface Area) somewhere in the field of 20 and 130 Å2, MW somewhere in the range of 150 and 500 g/mol, solubility: log S not higher than 6, flexibility: close to 9 rotatable bonds, and saturation: part of carbons in the sp3 hybridization at least 0.25) (Table 7).

Table 7. Physicochemical properties of the synthesized molecules **3 a-s** and standard drugs (MW: Molecular weight; HA: Heavy atoms; AHA: Aromatic heavy atom; FCsp3: Fraction Csp3; RTB: Rotatable bonds; HBA: H-bond acceptors; HBD: H-bond donors; MR: Molar refractivity; TPSA: Topological polar surface area; SD- Standard doxycycline; SF – Standard fluconazole)

Sr. No.	MW	HA	AHA	FCsp3	RTB	HBA	HBD	MR	TPSA
2a	324.4	23	17	0.11	5	4	0	94.23	71.95
2d	339.37	24	17	0.06	4	5	1	97.06	119.54
2m	428.13	23	17	0	3	3	1	100.99	73.72
2q	294.37	21	17	0.06	3	3	1	88.24	73.72
3a	407.45	29	17	0.2	6	7	0	109.88	129.65
3b	391.45	28	17	0.2	5	6	0	108.35	120.42
3c	404.49	29	17	0.24	5	5	0	116.07	114.43
3d	422.42	30	17	0.16	5	8	1	112.7	177.24
3e	407.45	29	17	0.2	5	7	1	110.37	140.65
3f	546.38	31	17	0.24	5	6	1	130.81	134.66
3g	499.38	31	17	0.24	5	6	1	125.79	134.66
3h	486.34	30	17	0.2	5	7	1	118.07	140.65
3i	490.76	29	17	0.16	4	6	1	116.59	131.42
3j	506.76	30	17	0.16	5	7	1	118.12	140.65
3k	432.28	28	17	0.11	4	6	1	108.94	131.42
3l	521.73	31	17	0.11	5	8	1	120.45	177.24
3m	511.18	29	17	0.11	4	6	1	116.64	131.42

3n	519.8	31	17	0.2	5	6	1	125.83	134.66
3o	397.84	27	17	0.11	4	6	1	103.93	131.42
3p	412.38	29	16	0.18	5	9	1	104.97	190.38
3q	377.42	27	17	0.16	4	6	1	103.88	131.42
3r	569.8	31	17	0.2	5	7	1	130.06	140.65
3s	566.8	31	17	0.2	5	6	1	130.85	134.66
SD	444.43	32	6	0.41	2	9	6	110.91	181.62
SF	306.27	22	16	0.23	5	7	1	70.71	81.65

By comparing the bioavailability radar between the Schiff base and the β-lactam (Fig. 10), it observed that the insaturation axes of the synthesized β-lactam decrease, but the polarity and insolubility range along the axes increase.

The drug resemblance properties of the fused compound and standard drug are articulated to by the red mutilated hexagon inside the pink shade (Figs. 11 and 12). The molecules fall within the drug-likeness parameter of a bioavailable drug are depicted in Table 8. SwissADME likewise has computational channels that incorporate Ghote et al. (1999), Egan et al. (2000), Veber et al. (2002) and Muegee et al. (2001) created by top pharmaceutical organizations and cheminfomaticians to assess the drug resemblance of molecules.

Table 8. The drug-likness ideal range for every property of a bioavailable drug. (Lipo- lipophilicity; Insolu. – Insolubility; Insatu. – Insaturation, IN – Inside the hexagon speaks; OUT – Outside the hexagon speaks, BOU- Boundary of the hexagon speaks)

Sr. No.	Flex	Lipo	Size	Polar	Insolu.	Insatu.
3a	IN	IN	IN	IN	IN	OUT
3b	IN	IN	IN	IN	IN	OUT
3c	IN	BOU	IN	IN	IN	BOU
3d	IN	IN	IN	OUT	IN	OUT
3e	IN	IN	IN	IN	IN	OUT
3f	IN	OUT	OUT	BOU	OUT	BOU
3g	IN	BOU	BOU	BOU	BOU	BOU
3h	IN	BOU	BOU	OUT	OUT	OUT
3i	IN	BOU	BOU	OUT	OUT	OUT
3j	IN	OUT	BOU	OUT	OUT	OUT
3k	IN	BOU	IN	BOU	BOU	OUT

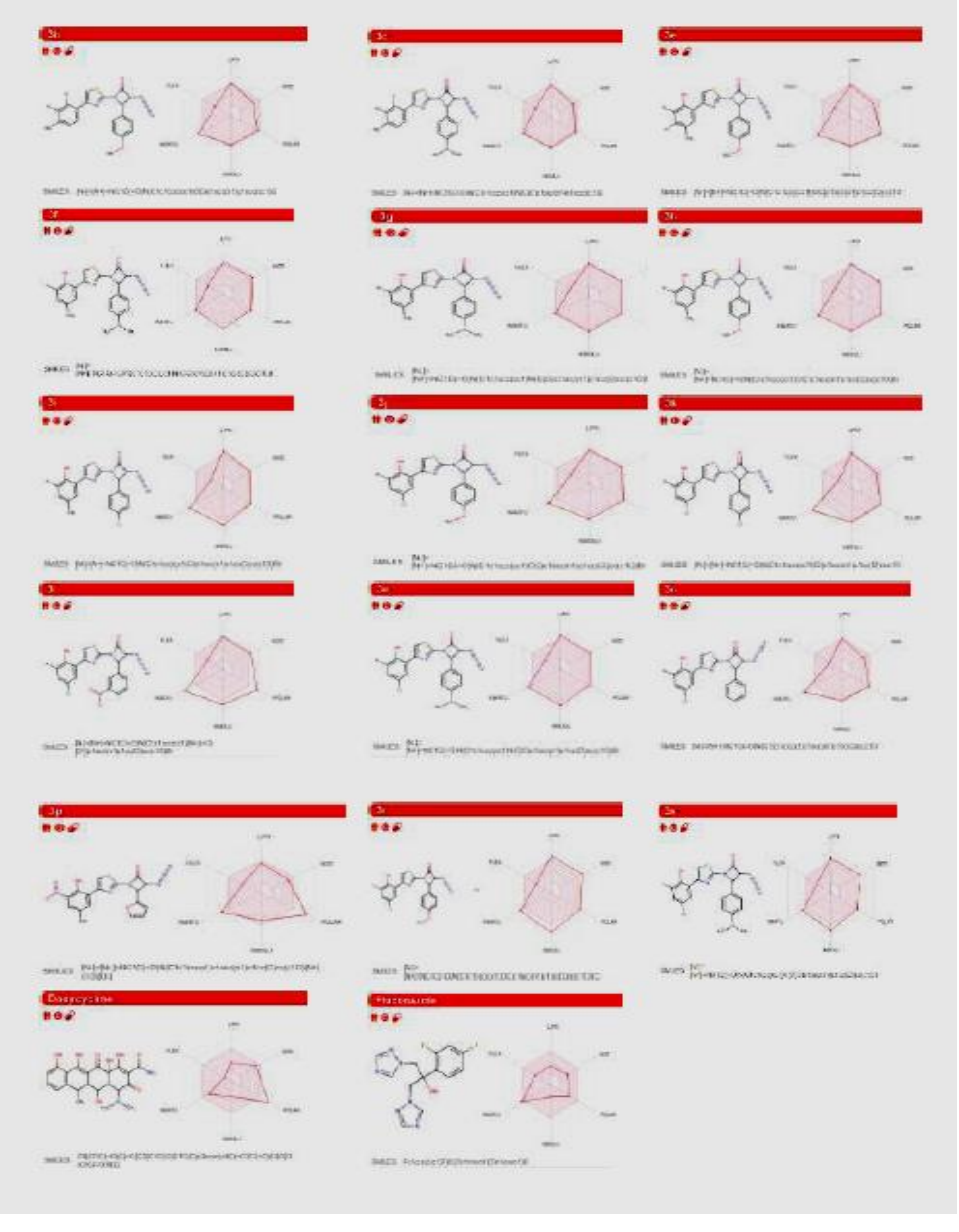

Figure 11. The bioavailability radar comparison between the synthesized molecules **2a,d,m,q** vs **3a,d,m,q** evaluating using swissADME web tool

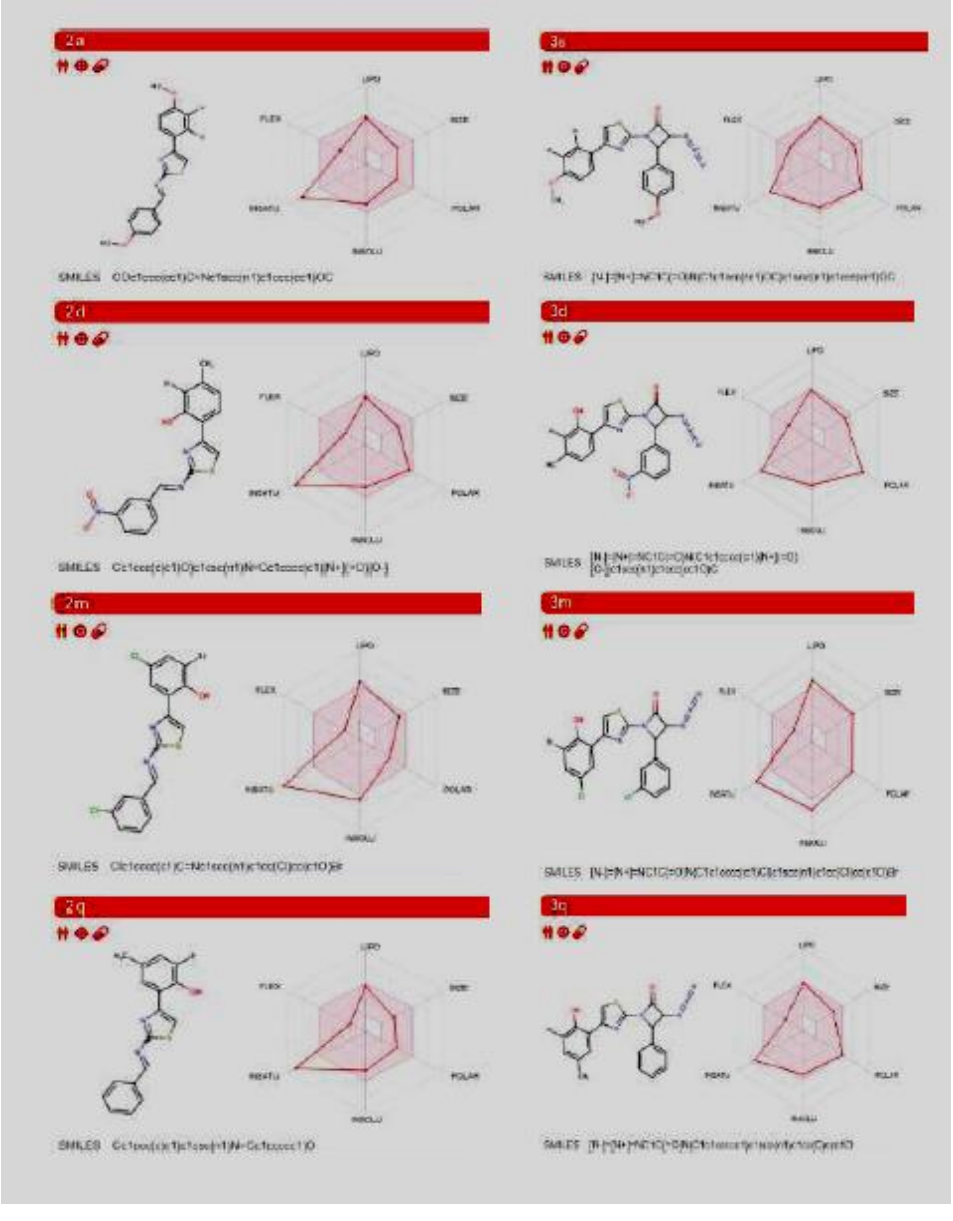

Figure 12. The bioavailability radar of the synthesized molecules (**3 b-s**) and standard drugs (Doxycycline, Fluconazole) evaluating using the swissADME web tool

3l	IN	OUT	OUT	OUT	OUT	OUT
3m	IN	OUT	BOU	BOU	OUT	OUT
3n	IN	OUT	BOU	BOU	OUT	OUT
3o	IN	IN	IN	IN	IN	OUT
3p	IN	IN	IN	OUT	IN	OUT
3q	IN	IN	IN	IN	IN	OUT
3r	IN	OUT	OUT	OUT	OUT	OUT
3s	IN	OUT	OUT	OUT	OUT	OUT
SD	IN	IN	IN	OUT	IN	IN
SF	IN	IN	IN	IN	IN	OUT

SD – Standard doxycycline; SF – Standard fluconazole

The Ghose screen quantitatively describes molecules dependent on figured physicochemical property profiles that incorporate log P, molar refractivity (MR), molecular weight (MW), and several atoms. The passing scope of determined log P (ClogP) is between – 0.4 and 5.6. For MW, the passing extent is somewhere in the range of 160 and 480. For MR, the passing reach is somewhere in the field of 40 and 130, and for the total number of atoms, the passing extent is between 20 and 70 atoms in a small molecule. Our compounds **2a, d, q,** while **3a-e, k, o, p, q**, and fluconazole standard tested to qualify the Ghose qualifying criteria, but the molecule **2m** and **3f-j, l-n, r** and **3s** out of the qualifying range (Table 9).

Table 9. Drug-likeness evaluation of synthesized compounds (**2a,d,m,q** and **3a-s**) using swissADME

Sr. No.	Lipinski #violations	Ghose #violations	Veber #violations	Egan #violations	Muegge #violations
2a	0	0	0	0	0
2d	0	0	0	0	0
2m	1	1	0	1	1
2q	0	0	0	0	0
3a	0	0	0	0	0
3b	0	0	0	0	1
3c	0	0	0	0	1
3d	0	0	1	1	1
3e	0	0	1	1	0
3f	1	2	0	1	1

3g	0	1	0	1	1
3h	0	1	1	1	1
3i	0	1	0	0	1
3j	1	1	1	1	1
3k	0	0	0	0	1
3l	1	1	1	1	2
3m	1	2	0	0	1
3n	1	1	0	1	1
3o	0	0	0	0	1
3p	1	0	1	1	1
3q	0	0	0	0	0
3r	1	2	1	1	1
3s	1	2	0	1	1
SD	1	1	1	1	2
SF	0	0	0	0	0

SD – Standard doxycycline; SF – Standard fluconazole

Veber (GSK) filter model represents molecules as druglike on the off chance that they have ten or less rotatable bonds and a PSA equivalent to or under 140 Å with 12 or less H-bond donors and acceptors.

Egan (Pharmacia) filter gives an expectation of drug assimilation dependent on physical procedures engaged with film absorbency of a molecule. Significantly, the Egan computational model for human passive intestinal absorption (HIA) of molecule represents dynamic carriage and efflux components and is, in this way, vigorous in foreseeing adaptation of drugs. The Egan violation only observed in **2m; 3d-h, j,l,n,p,r-s,** and the doxycycline standard drug (Table 9).

Muegge (Bayer filter) model is a database-free pharmacophore point screen that separates between druglike and nondrug-like matter. It depends on the perception that non-drugs are frequently less functionalized. Four purposeful themes characterized to be significant in druglike molecules and incorporate hydroxyl, amine, ketone, and sulfonyl groups. In this manner, a base check of well-characterized pharmacophore focuses is required to pass the screen. The manifestation of these efficient themes ensures hydrogen-holding capacities that are basic for explicit drug cooperation with its objectives. These serviceable groups can consolidate to what the Muegge model alludes to as pharmacophore points. The pharmacophore emphases incorporate amine, amide, alcohol, ketone, sulfone, sulfonamide, carboxylic acid, carbamate, guanidine, amidine, urea, and active ester groups. These pharmacophore efforts in molecules possibly give critical communications with the

objective protein. From the screening data, the synthesized compound **2m** and **3b-d, f-p, r-s** along with doxycycline that they don't have the recommended functional group for the interaction with the target protein suggested by the Muegge.

PAINS, Break and Leadlikeness screening

PAINS (pan-assay interference screening) that often gives false favorable chemical properties results in high-throughput screens. PAINS tend to react non-specifically with numerous biological targets rather than specifically affecting one anticipated goal.

PAINS (pan-assay interference screening) that regularly give false favorable synthetic properties bring about high-throughput screens. PAINS will, in general, respond non-specifically with various biological targets as opposed to explicitly influencing one anticipated objective.

SwissADME evaluation did not post any PAINS alert except **2a, d, m, q**, and standard doxycycline and fluconazole molecules (Table 10).

In another choice model, Brenk et al. (2008) considered composites that are smaller and less hydrophobic and not those characterized by "Lipinski's standard of 5" to enlarge open doors for lead streamlining. After the prohibition of compounds with possibly mutagenic, reactive, and unfavorable groups, for example, nitro, sulfates, phosphates, 2-halopyridines, and thiols. Brenk model confines the ClogP/ClogD to sandwiched between zero and four, the quantity of hydrogen-bond donors and acceptors to less than 4 and 7, individually, and the number of substantial atoms to in the range of 10 and 27. Furthermore, just compounds with restricted entanglement characterized as less than eight rotatable bonds, less than five ring structures, and no ring structures with more than two fused rings are considered medicinal. The **2a, d, m, q** with all the β-lactams derivatives and standard doxycycline flouted break rule.

Leadlikeness tests proposed to furnish leads with great kinship in high-throughput screens that take into account the detection and manipulation of new exchanges in the lead advancement stage (Table 10). Only the standard fluconazole drugs passed all the leadlikness criteria, while all the synthesized compounds with the standard doxycycline fail in leadlikness.

Table 10. Medicinal chemistry evaluation of the synthesized compounds

Sr. No.	PAINS #alerts	Brenk #alerts	Leadlikeness #violations	Synthetic Accessibility
2a	0	1	1	3.12
2d	0	3	1	3.19
2m	0	1	2	3.1
2q	0	1	1	3.14

3a	1	3	2	3.82
3b	1	3	2	3.79
3c	3	3	2	3.95
3d	1	5	2	3.89
3e	1	3	2	3.91
3f	3	4	2	4.15
3g	3	3	2	4.12
3h	1	3	2	3.99
3i	1	3	2	3.87
3j	1	3	2	3.86
3k	1	3	2	3.66
3l	1	5	2	3.86
3m	1	3	2	3.77
3n	3	3	2	3.99
3o	1	3	2	3.64
3p	1	5	2	4.09
3q	1	3	2	3.79
3r	1	4	2	4.07
3s	3	4	2	4.01
SD	0	1	1	5.25
SF	0	0	0	2.91

SD – Standard doxycycline; SF – Standard fluconazole

P-glycoprotein and CYP enzyme activity prediction

SwissADME additionally empowers the estimation for a compound to be a substrate of p-glycoprotein (P-gp) or inhibitor of the cytochrome p450 isoenzymes (CYP isoenzymes). P-gp is broadly dispersed and communicated in the intestinal epithelium where it thrusts xenobiotics, for example, medicates over into the intestinal lumen and in the delicate endothelial cells making the blood-brain barrier where it propels them once again into the vessels. CYP isoenzymes are in charge of the biotransformation of drugs (Ogu & Maxa, 2000). Drug digestion through CYP isoenzymes is a significant determinant of drug connections that can prompt to drug toxicities and diminished pharmacological impact. The models return “Yes“ or “No“ if the molecule under examination has a higher likelihood to be substrate or non-substrate of P-gp or inhibitor or non-inhibitor of a given CYP. The screening results tabulated (Table 11).

Table 11. Pharmacokinetic evaluation of the synthesized compounds (GI-abs.: gastrointestinal absorption; BBBper.: blood-brain barrier permeant; CYP: Cytochromes, P – gp sub: P – glycoprotein substrate)

Sr. No.	GI abs.	BBB per.	P-gp sub.	CYP1A2 inhibitor	CYP2C19 inhibitor	CYP2C9 inhibitor	CYP2D6 inhibitor	CYP3A4 inhibitor
2a	High	Yes	No	Yes	Yes	Yes	No	Yes
2d	High	No	No	Yes	Yes	Yes	No	No
2m	High	No	No	Yes	Yes	Yes	No	No
2q	High	No	No	Yes	Yes	Yes	No	No
3a	Low	No	No	Yes	Yes	Yes	No	Yes
3b	High	No	No	Yes	Yes	Yes	No	Yes
3c	High	No	No	No	Yes	Yes	No	Yes
3d	Low	No	No	No	Yes	Yes	No	No
3e	Low	No	No	Yes	Yes	Yes	No	Yes
3f	Low	No	No	No	Yes	Yes	No	No
3g	Low	No	No	No	Yes	Yes	No	Yes
3h	Low	No	No	Yes	Yes	Yes	No	No
3i	Low	No	No	Yes	Yes	Yes	No	No
3j	Low	No	No	Yes	Yes	Yes	No	No
3k	Low	No	No	Yes	Yes	Yes	No	No
3l	Low	No	No	Yes	Yes	Yes	No	No
3m	Low	No	No	Yes	Yes	Yes	No	No
3n	Low	No	No	No	Yes	Yes	No	No
3o	Low	No	No	Yes	Yes	Yes	No	No
3p	Low	No	No	No	Yes	Yes	No	No
3q	Low	No	No	Yes	Yes	Yes	No	No
3r	Low	No	Yes	No	Yes	No	No	No
3s	Low	No	No	No	Yes	Yes	No	No
SD	Low	No	Yes	No	No	No	No	No
SF	High	No	No	No	Yes	No	No	No

SD – Standard doxycycline; SF – Standard fluconazole

HIA and BBB prediction

Appropriate to P-gp and CYP protein energy is human gastrointestinal ingestion (HIA) and blood-brain barrier infiltration (BBB). SwissADME 'BOILEDegg' (Fig. 13) permits for assessment of HIA as an element of the

situation of the molecules in the WLOGP-versus-TPSA referential. The white section of the 'BOILEDegg' is for a high possibility of reflexive adaptation by the gastrointestinal tract, and the yellow area (yolk) is for a high probability of cerebrum entrance, which is shown by all the Schiff base while all the β-lactams are out of the region. Yolk and white zones are not fundamentally unrelated. With this, the points are shaded in blue whenever anticipated as effectively effluxed by P-gp (PGP+) and in red predicted as non-substrate of P-gp (PGP−).

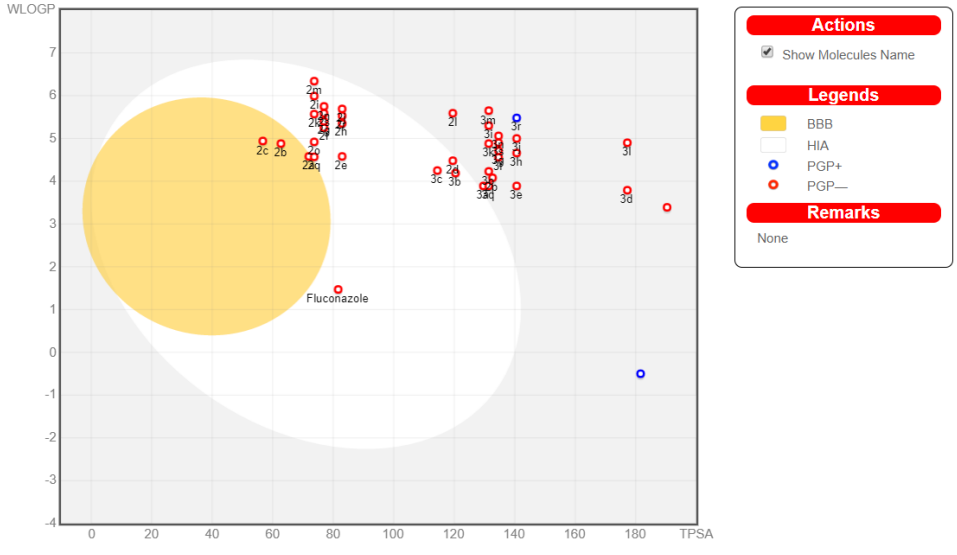

Figure 13. The BOILED-Egg allows for evaluation of passive gastrointestinal absorption (HIA), brain penetration (BBB) and P-glycoprotein in the presence of the molecule (P-gp)

HIA and BBB are subject to water solubility and lipophilicity of the drug. Two topological approaches to foresee water solubility comprised of SwissADME. The first is an execution of the ESOL (Delaney, 2004) model, and the subsequent one modified by Fagerberg et al. (2015). SILICON-IT created SwissADME third indicator for solubility. All anticipated qualities are the decimal logarithm of the molar solubility in water (log S).

The ESOL, Ali, and Silicons IT screening solubility of all the synthesized compounds depicted in Table 12. Even the standard drugs are in the range of solubility to very soluble. Consensus Log p is the average value of all Log P evaluated with various lipophilicity criteria (Table 13).

Table 12. Water solubility evaluation of the synthesized compounds. (Solu: Solubility; PS: Poorly soluble; MS: Moderately soluble; S: soluble; VS: Very soluble)

Sr. No.	ESOL				Ali				Silicos			
	Log S	Solubility (mg/ml)	Solubility (mol/l)	Class	Log S	Solubility (mg/ml)	Solubility (mol/l)	Class	Log S	Solubility (mg/ml)	Solubility (mol/l)	Class
2a	-4.92	3.94E-03	1.21E-05	MS	-5.75	5.73E-04	1.77E-06	MS	-6.65	7.21E-05	2.22E-07	PS
2d	-4.78	5.62E-03	1.66E-05	MS	-6.31	1.68E-04	4.95E-07	PS	-5.58	8.91E-04	2.62E-06	MS
2m	-6.52	1.29E-04	3.00E-07	PS	-7.16	2.97E-05	6.93E-08	PS	-7.83	6.38E-06	1.49E-08	PS
2q	-4.75	5.24E-03	1.78E-05	MS	-5.52	8.89E-04	3.02E-06	MS	-6.22	1.75E-04	5.96E-07	PS
3a	-5.36	1.78E-03	4.38E-06	MS	-7.14	2.95E-05	7.23E-08	PS	-6.24	2.36E-04	5.79E-07	PS
3b	-5.59	1.01E-03	2.59E-06	MS	-7.35	1.74E-05	4.45E-08	PS	-6.51	1.21E-04	3.09E-07	PS
3c	-5.75	7.15E-04	1.77E-06	MS	-7.39	1.64E-05	4.06E-08	PS	-6.48	1.33E-04	3.30E-07	PS
3d	-5.44	1.53E-03	3.63E-06	MS	-8.04	3.89E-06	9.20E-09	PS	-5.16	2.92E-03	6.92E-06	MS
3e	-5.45	1.45E-03	3.55E-06	MS	-7.41	1.57E-05	3.86E-08	PS	-5.92	4.88E-04	1.20E-06	MS
3f	-6.79	8.92E-05	1.63E-07	PS	-8.12	4.17E-06	7.63E-09	PS	-6.71	1.08E-04	1.97E-07	PS
3g	-6.52	1.50E-04	3.01E-07	PS	-8.16	3.46E-06	6.93E-09	PS	-6.66	1.08E-04	2.17E-07	PS
3h	-6.36	2.13E-04	4.37E-07	PS	-8.13	3.61E-06	7.43E-09	PS	-6.7	9.82E-05	2.02E-07	PS
3i	-6.88	6.43E-05	1.31E-07	PS	-8.62	1.18E-06	2.40E-09	PS	-7.18	3.25E-05	6.62E-08	PS
3j	-6.65	1.14E-04	2.24E-07	PS	-8.4	2.02E-06	3.99E-09	PS	-6.9	6.37E-05	1.26E-07	PS
3k	-6.26	2.35E-04	5.43E-07	PS	-8.17	2.90E-06	6.70E-09	PS	-6.62	1.05E-04	2.42E-07	PS
3l	-6.64	1.19E-04	2.29E-07	PS	-9.02	4.96E-07	9.50E-10	PS	-6.13	3.82E-04	7.33E-07	PS
3m	-7.17	3.43E-05	6.71E-08	PS	-8.89	6.58E-07	1.29E-09	PS	-7.38	2.11E-05	4.13E-08	PS
3n	-6.81	8.02E-05	1.54E-07	PS	-8.43	1.94E-06	3.73E-09	PS	-6.87	7.03E-05	1.35E-07	PS
3o	-5.67	8.48E-04	2.13E-06	MS	-7.52	1.20E-05	3.02E-08	PS	-6.03	3.70E-04	9.31E-07	PS
3p	-5.15	2.94E-03	7.14E-06	MS	-7.95	4.64E-06	1.12E-08	PS	-4.38	1.70E-02	4.13E-05	MS
3q	-5.38	1.57E-03	4.16E-06	MS	-7.25	2.12E-05	5.62E-08	PS	-5.82	5.73E-04	1.52E-06	MS
3r	-7.41	2.21E-05	3.88E-08	PS	-9.03	5.29E-07	9.29E-10	PS	-6.94	6.51E-05	1.14E-07	PS
3s	-7.08	4.74E-05	8.36E-08	PS	-8.39	2.32E-06	4.10E-09	PS	-6.91	6.99E-05	1.23E-07	PS
SD	-2.94	5.07E-01	1.14E-03	S	-3.93	5.28E-02	1.19E-04	S	-1.37	1.88E+01	4.24E-02	S
SF	-2.17	2.08E+00	6.80E-03	S	-1.63	7.20E+00	2.35E-02	VS	-3.54	8.83E-02	2.88E-04	S

SD – Standard doxycycline; SF – Standard fluconazole

Table 13. Lipophilicity evaluation of the synthesized compounds

Sr. No.	iLOGP	XLOGP3	WLOGP	MLOGP	Silicos-IT Log P	Consensus Log P
2a	3.63	4.52	4.58	2.62	5.59	4.19
2d	2.86	4.09	4.48	1.95	3.35	3.35
2m	3.66	5.84	6.34	4.36	6.97	5.43
2q	3.23	4.26	4.57	2.97	5.54	4.12
3a	3.65	4.69	3.89	2.1	2.9	3.45
3b	3.38	5.08	4.19	2.62	3.36	3.73
3c	3.44	5.24	4.25	2.85	2.98	3.75
3d	2.7	4.59	3.79	1.54	0.67	2.66
3e	3.35	4.73	3.89	2.1	2.88	3.39
3f	3.64	5.53	4.56	3.03	3.48	4.05
3g	3.57	5.57	4.71	2.92	3.19	3.99
3h	3.58	5.42	4.66	2.7	3.56	3.99
3i	3.51	6.08	5.3	3.49	4.15	4.51
3j	3.57	5.68	5	2.97	3.69	4.18
3k	3.38	5.65	4.88	3.16	3.6	4.13
3l	2.95	5.54	4.9	2.42	1.49	3.46
3m	3.44	6.34	5.65	3.76	4.28	4.69
3n	3.47	5.83	5.06	3.19	3.31	4.17
3o	3.01	5.02	4.23	2.66	2.96	3.58
3p	2.07	4.24	3.39	0.35	0.08	2.02
3q	3.04	4.76	3.89	2.4	2.83	3.38
3r	0	6.29	5.48	3.3	3.98	3.81
3s	3.54	5.79	4.9	3.3	3.6	4.23
SD	1.93	0.54	-0.5	-2.08	-0.98	-0.22
SF	0.41	0.35	1.47	1.47	0.71	0.88

SD – Standard doxycycline; SF – Standard fluconazole

Experimental

General

Every one of the reactions was conveyed under the stipulated conditions, utilizing freshly prepared thiazole, ionic liquid, and pure solvents. The open capillary technique was used to decide the melting point of the compound and are uncorrected. The refined dissolvable was utilized to perform TLC on silica gel G. All

the chemicals were obtained from SD. Fine chemicals of AR grade. ^{1}H NMR and ^{13}C NMR spectra recorded from DMSO-d_6 solutions on a Brucker AC 400 (MHz). TMS as an internal standard for detailing the chemical shift in ^{1}H NMR. KBr discs method used to IR spectra on a Perkin Elmer 1800 spectrophotometer and mass spectra portrayal finished with a GC-MS (70ev). All tertiary alkyl amines concentrated H_2SO_4, cyclohexanone, and aromatic aldehydes bought from SD. Fine chemicals of AR grades.

Synthesis of N-(4-methoxybenzylidene)-4-(4-methoxyphenyl) thiazol-2-amine (2a)

N-(4-methoxybenzylidene)-4-(4-methoxyphenyl) thiazol-2-amine was synthesized by the reaction between 4-(4-methoxyphenyl) thiazol-2-amine and anisaldehyde in the presence of conc.H_2SO_4 in ethanolic medium gives the desired product. The yield was 87%. M.P.: 187 ^{0}C; IR (KBr): ν_{max}cm^{-1} 1610, 771, 2930cm^{-1}; ^{1}H-NMR: δ 8.12 (1H, s), 7.12-7.18 (2H, d), 7.16-7.18 (2H, d), 6.88-6.90 (2H, d), 6.69-6.71 (2H, d), 5.61 (1H, s), 3.75 (6H, s)

Synthesis of 3-azido-4-(4methoxyphenyl)-1-(4-(4-methoxyphenyl thiazol-2-yl) azetidin-2-one 3a

To a 10 mL round bottom flask containing ionic liquid [bmim][PF_6] (3.0 mL) and 1 mL of [Et_3NH]$^{+}$[HSO_4]$^{-}$, N-(4-methoxybenzylidene)-4-(4-methoxyphenyl) thiazol-2-amine, **2a** (0.13mmol) was added. The reaction mixture was stirred at RT for 15 min. azidoacetic acid (0.13mmol) was added to the reaction mixture and continued stirring for 4 hours at 45-50^{0}C. After completion of the reaction (monitored by TLC), the solid product obtained triturated with solvent ether in 3 fractions (3x5mL). The organic layer was evaporated under reduced pressure to get the ionic liquid back for reuse. The resulting product was dried and purified by crystallized from alcohol, acetic acid; to furnish the product in yield was 75%.

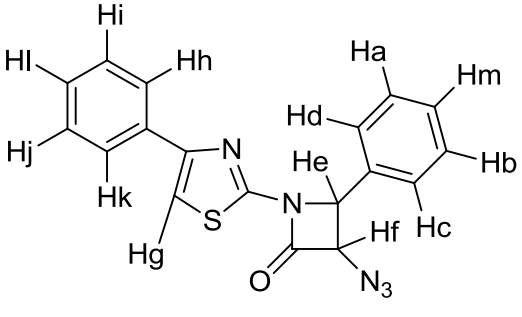

M.P.: 138 ^{0}C; IR (KBr): ν_{max}cm^{-1} 3000, 2930, 2124, 1720 cm^{-1}; ^{1}H-NMR : δ 3.75 (s, 6H, Ar-$(OCH_3)_2$), 5.63-5.68 (d, 1H, *J* 18.84Hz, He), 6.24-6.24 (d, 1H, *J* 13.52Hz,

Hf), 6.64-6.66 (d, 2H, *J* 8.64Hz, Ha,b), 6.81-6.83 (d, 2H, *J* 8.76Hz, Hj,k), 7.15-7.21 (d, 4H, Hc,d,k,h), 7.67 (s, 1H, Hg); ^{13}C NMR : δ 56.92, 70.66, 71.61, 80.93, 84.73, 98.21, 117.37, 119.12, 129.16, 136.31, 138.09, 142.04, 146.81, 163.75, 165.0-168.75, 170.18; **MS** (m/z) : (407.1M$^+$); Elemental Analysis ($C_{20}H_{17}N_5O_3S$): Calculated: C: 58.96, H: 4.21, N: 17.19; Found: C: 58.24, H: 4.19, N: 17.12

All compounds were prepared by the aforementioned procedure; all reactions were monitored by TLC after specified times.

3-azido-4-(4-methoxyphenyl)-1-(4-p-tolyithiazol-2-yl)azetidin-2-one 3b

M.P.: 205 ^{0}C; IR (KBr): ν_{max}cm^{-1} 3110, 2098, 1690, 780cm^{-1}; ^{1}H-NMR : δ 2.38 (s, 3H, Ar-CH_3), 3.78 (s, 3H, Ar-OCH_3), 5.80-5.83 (d, 1H, *J* 10.92Hz, He), 6.36 (d, 1H, *J* 6Hz, Hf), 7.44 (s, 1H, Hg), 7.50-7.52 (d, 2H, *J* 6.72Hz, Ha,b), 7.63-7.70 (d, 2H, Hi,j), 7.81-7.94 (d, 4H, Hc,d,h,k); ^{13}C NMR : δ 22.3, 57.8, 59.3, 65.2, 100.2, 115.7, 127.1, 127.8, 130.1, 136.3, 138.5, 148.2, 158.2, 161.2, 162.3; MS (m/z) : (391.1M$^+$); Elemental Analysis ($C_{20}H_{17}N_5O_2S$) : Calculated: C: 61.37, H: 4.38, N: 17.89; Found: C: 61.21, H: 4.32, N: 17.78.

3-azido-4-(4-(dimethylamino)phenyl)-1-(4-p-tolylthiazol-2-yl)azetidin-2-one 3c

M.P.: 230 ^{0}C; IR (KBr): ν_{max}cm^{-1} 2997, 2980, 2111, 1697, 1340, 762cm^{-1}; ^{1}H-NMR : δ 2.79 (s, 3H, Ar-CH_3), 2.99 (s, 6H, Ar-N$(CH_3)_2$), 5.40-5.42 (d, 1H, *J* 8.92Hz, He), 5.78-5.79 (d, 1H, *J* 2.68Hz, Hf), 6.58 (s, 1H, Hg), 6.68-6.70 (d, 2H, *J* 8.04Hz, Ha,b), 7.10-7.12 (d, 2H, *J* 7.96Hz, Hi,j), 7.36-7.38 (d, 2H, *J* 8.04Hz, Hc,d), 7.65-7.66 (d, 2H, *J* 3.68Hz, Hk,h); ^{13}C NMR : δ 24.2, 40.2, 59.4, 66.7, 101.2, 114.3, 128.6, 129.9, 130.7, 131.3, 138.6, 149.2, 149.8, 161.5; MS (m/z) : (404M$^+$); Elemental Analysis ($C_{21}H_{20}N_6OS$) : Calculated: C: 62.86, H: 4.98, N: 20.78; Found: C: 62.81, H: 4.98, N: 20.73

3-azido-4-(3-nitrophenyl)-1-(4-p-tolylthiazol-2-yl)azetidin-2-one 3d

M.P.: 170 ^{0}C; IR (KBr): ν_{max}cm^{-1} 2990, 2087, 1692, 1080, 790cm^{-1}; ^{1}H-NMR : δ 2.00 (s, 3H, Ar-CH_3), 5.48-5.49 (d, 1H, *J* 1.72Hz, He), 5.96-5.98 (d, 1H, *J* 8.4Hz, Hf), 6.50 (s, 1H, Hg), 6.68-6.70 (d, 1H, *J* 8.04Hz), 6.90-6.91 (d, 2H, *J* 4.6Hz, Hi,j), 7.48-7.49 (d, 3H, *J* 4.12Hz, Hc,b,m), 7.65-7.66 (d, 2H, *J* 5.2Hz, Hk,h); ^{13}C NMR : δ 23.1, 58.2, 64.7, 99.3, 119.7, 123.6, 128.7, 131.4, 132.2, 134.6, 139.8, 145.5, 149.6, 163.2; MS (m/z) : (406.08M$^+$); Elemental Analysis ($C_{19}H_{14}N_6O_3S$): Calculated: C: 56.15, H: 3.47, N: 20.68; Found: C: 56.13 , H: 3.45, N: 20.61.

3-azido-1-(4-(2-hydroxy-5-methylphenyl)thiazol-2-yl)4-(4-methoxyphenyl) azetidin-2-one 3e

M.P.: 170 ^{0}C; IR (KBr): ν_{max}cm^{-1} 3100, 2990, 2109, 1962, 680cm^{-1}; ^{1}H-NMR : δ 2.77 (s, 3H, Ar-CH_3), 3.76 (s, 3H, Ar-OCH_3), 5.55-5.58 (d, 1H, *J* 15.08Hz,

Hf), 6.87-6.89 (d, 1H, *J* 5.16Hz, He), 6.50 (s, 1H, Hg), 6.68-6.70 (d, 2H, *J* 8.04Hz, Ha,b), 6.90-6.91 (d, 2H, *J* 4.6Hz, Hc,d), 7.39-7.49 (t, 1H, Hl), 7.65-7.66 (d, 1H, *J* 5.2Hz, Hi), 7.82 (s, 1H, Hk), 9.15 (s, 1H, Ar-OH); ^{13}C NMR : δ 25.1, 57.2, 59.8, 66.7, 99.7, 115.5, 118.8, 121.3, 127.4, 132.1134.5, 138.2, 149.3, 154.3, 159.6, 161.8; **MS** (m/z) : (407.11M$^+$); Elemental Analysis ($C_{20}H_{17}N_5O_3S$): Calculated: C: 58.96, H: 4.4, N: 17.19; Found: C: 58.95, H: 4.38, N: 17.14.

3-azido-4-(4-(dimethylamino)phenyl)-1-(4-(2hydroxy-3-iodo-5-methylphenyl) thiazol-2-yl)azetidin-2-one 3f

M.P.: 186 ^{0}C; IR (KBr): ν_{max}cm^{-1} 3120, 2999, 2112, 769cm^{-1}; ^{1}H-NMR : δ 2.32 (s, 3H, Ar-CH_3), 2.80 (s, 6H, Ar-N(CH_3)$_2$), 5.49-5.50 (d, 1H, *J* 3.12Hz, Hf), 5.82-5.83 (d, 1H, *J* 6.4Hz, He), 6.58 (s, 1H, Hg), 6.68-6.70 (d, 2H, *J* 8.04Hz, Ha,b), 7.10-7.12 (d, 2H, *J* 7.96Hz, Hc,d), 7.36-7.38 (d, 1H, *J* 8.04Hz, Hl), 7.65-7.66 (d, 1H, *J* 3.68Hz, Hk), 8.82 (s, 1H, Ar-OH); ^{13}C NMR : δ 25.5, 41.2, 60.3, 65.1, 88.6, 102.1, 115.6, 124.2, 128.3, 132.2, 135.5, 140.2, 148.1, 1149.5, 160.1, 162.3; MS (m/z) : (546M$^+$); Elemental Analysis ($C_{21}H_{19}IN_6O_2S$) : Calculated: C: 46.16, H: 3.51, N: 15.38; Found: C: 46.14, H: 3.50, N: 15.31.

3-azido-1-(4-(3-bromo-2-hydroxy-5-methylphenyl)thiaazol-2-yl)-4(4 (dimethyl-amino)phenyl)azetidin-2-one 3g

M.P.: 100 ^{0}C; IR (KBr): ν_{max}cm^{-1} 3110, 2098, 1701, 1390, 724, 670cm^{-1}; ^{1}H-NMR : δ 2.16 (s, 3H, Ar-CH_3), 4.15 (s, 6H, Ar-N(CH_3)$_2$), 5.15-5.18 (d, 1H, *J* 13.92Hz, He), 5.75-5.76 (d, 1H, *J* 5.00Hz, Hf), 7.20-7.20 (d, 2H, *J* 2.68Hz), 7.38-7.41 (q, 2H), 7.62 (s, 1H, Hg), 7.73-7.77 (d, 1H, *J* 5.00Hz, Hk), 7.85-7.87 (d, 1H, *J* 9.2Hz, Hl), 11.96 (s, 1H, Ar-OH); ^{13}C NMR : δ 26.4, 40.3, 59.8, 67.3, 101.2, 115.3, 125.1, 129.5, 131.2, 136.2, 136.9, 138.5, 149.2, 150.5, 153.3, 162.1; MS (m/z) : (500.05M$^+$); Elemental Analysis ($C_{21}H_{19}BrN_6O_2S$) : Calculated: C: 50.51, H: 3.85, N: 16.83; Found: C: 50.48, H: 3.82, N: 16.82.

3-azido-1-(4-(3-bromo-2-hydroxy-5-methylphenyl)thiaazol-2-yl)-4(4-methoxy-phenyl) azetidin-2-one 3h

M.P.: 230 ^{0}C; IR (KBr): ν_{max}cm^{-1} 3012, 2991, 2108, 1590, 1690, 735, 680cm^{-1}; ^{1}H-NMR : δ 2.35 (s, 3H, Ar-CH_3), 4.10 (s, 3H, Ar-OCH_3), 5.44-5.47 (d, 1H, *J* 13.56Hz, He), 6.18-6.19 (d, 1H, *J* 6.12Hz, Hf), 7.58-7.59 (d, 2H, *J* 3.12Hz, Ha,b), 7.63-7.64 (d, 2H), 7.85-7.86 (d, 1H, *J* 4.64Hz, Hl), 8.01-8.04 (d, 1H, *J* 9.8Hz, Hk), 8.27 (s, 1H, Hg), 12.21 (s, 1H, Ar-OH); ^{13}C NMR : δ 21.1, 57.3, 59.8, 64.1, 99.8, 116.3, 124.3, 128.7, 130.3, 133.5, 138.9, 139.2, 149.8, 152.4, 159.8, 161.2; MS (m/z) : (487.01M$^+$); Analysis ($C_{20}H_{16}BrN_5O_3S$) : Calculated: C: 49.39, H: 3.32, N: 14.40; Found: C: 49.35, H: 3.30, N: 14.38.

3-azido-1-(4-(3-bromo-2-hydroxy-5-methylphenyl)thiaazol-2-yl)-4(4-chlorophenyl) azetidin-2-one 3i

M.P.: 94 ^{0}C; IR (KBr): ν_{max}cm^{-1} 3440, 3105, 2089, 1710, 682.1cm^{-1}; ^{1}H-NMR : δ 2.16 (s, 3H, Ar-CH_3), 5.39-5.40 (d, 1H, *J* 4.36Hz, He), 6.00-6.02 (d, 1H, *J* 10.68Hz, Hf), 7.31 (s, 1H, Hg), 7.62-7.64 (d, 2H, *J* 8.36Hz, Ha,b), 7.75-7.76 (d, 2H, *J* 6.4Hz, Hc,d), 7.87-7.88 (d, 1H, *J* 2.96Hz, Hl), 8.21-8.25 (d, 1H, *J* 15.52Hz, Hk), 12.13 (s, 1H, Ar-OH); ^{13}C NMR : δ 23.7, 58.1, 65.7, 102.1, 114.2, 124.3, 129.9, 132.7, 134.4, 136.8, 138.5, 144.3, 149.8, 153.0, 162.2; MS (m/z) : (490.96M$^+$); Elemental Analysis ($C_{19}H_{13}BrClN_5O_2S$) : Calculated: C: 46.50, H: 2.67, N: 14.27; Found: C: 46.48, H: 2.65, N: 14.26.

3-azido-1-(4-(3-bromo-5-chloro-2-hydroxyphenyl)thiaazol-2-yl) -4(4-methoxyphenyl) azetidin-2-one 3j

M.P.: 135 ^{0}C; IR (KBr): ν_{max}cm^{-1} 3500, 2067, 1530, 1340, 721, 675cm^{-1}; ^{1}H-NMR : δ 4.15 (s, 3H, Ar-OCH_3), 5.41-5.42 (d, 1H, *J* 5.12Hz, He), 5.71-5.72 (d, 1H, *J* 3.28Hz, Hf), 7.58-7.59 (d, 2H, *J* 4.04Hz, Ha,b), 7.61-7.62 (d, 2H, *J* 1.16Hz, Hc,d), 8.01-8.04 (d, 1H, *J* 1.92Hz, Hl), 8.12-8.15 (d, 1H, *J* 2.08Hz, Hk), 8.27 (s, 1H, Hg), 11.50 (s, 1H, Ar-OH); ^{13}C NMR : δ 55.9, 60.0, 85.3, 100.2, 114.1, 115.7, 124.2, 127.8, 128.9, 129.6, 131.9, 135.8, 148.2, 153.0, 158.7, 160.4; MS (m/z): (506.96M$^+$); Elemental Analysis ($C_{19}H_{13}BrClN_5O_3S$) : Calculated: C: 45.03, H: 2.59, N: 13.82; Found: C: 45.02, H: 2.53, N: 13.80.

3-azido-1-(4-(5-chloro-2-hydroxyphenyl)thiazol-2-yl)-4-(4-chlorophenyl) azetidin-2-one 3k

M.P.: 110 ^{0}C; IR (KBr): ν_{max}cm^{-1} 3480, 2089, 1603, 1645, 1010, 767cm^{-1}; ^{1}H-NMR : δ 5.25-5.26 (d, 1H, *J* 4.24Hz, Hf), 5.89-5.92 (d, 1H, *J* 10.58Hz, He), 6.68-6.70 (d, 2H, *J* 8.00Hz, Ha,b), 6.89-6.91 (d, 2H, *J* 8.8Hz, Hc,d), 7.12-7.38 (m, 2H, Hi,l), 7.65-7.66 (d, 1H, *J* 4.28Hz, Hk), 7.98 (s, 1H, Hg), 9.01 (s, 1H, Ar-OH); ^{13}C NMR : δ 61.2, 64.2, 101.2, 118.9, 123.4, 128.4, 129.8, 132.3, 134.8, 144.5, 149.7, 155.6, 163.7; MS (m/z) : (431.00M$^+$); Elemental Analysis ($C_{18}H_{11}Cl_2N_5O_2S$) : Calculated: C: 50.01, H: 2.56, N: 16.20; Found: C: 50.01, H: 2.47, N: 16.18.

3-azido-1-(4-(3-bromo-5-chloro-2-hydroxyphenyl)thiazol-2-yl)-4-(4-nitrophenyl) azetidin-2-one 3l

M.P.:140 ^{0}C; IR (KBr): ν_{max}cm^{-1} 3477, 2101, 1640, 700cm^{-1}; ^{1}H-NMR : δ 5.02-5.21 (d, 1H, *J* 5.68Hz, He), 5.84-5.86 (d, 1H, *J* 8.00Hz, Hf), 6.84-6.85 (d, 1H, *J* 4.48Hz, Hk), 7.16-7.38 (m, 4H, Hc,b,m), 7.65-7.66 (d, 1H, *J* 4.28Hz, Hl), 7.98 (s, 1H, Hg), 9.17 (s, 1H, Ar-OH); ^{13}C NMR : δ 57.8, 67.2, 103.2, 117.3, 118.1, 124.2, 125.2, 128.2, 130.5, 134.5136.7, 147.6, 149.2, 155.3, 160.1; MS (m/z) : (521.9M$^+$); Elemental Analysis ($C_{18}H_{10}BrClN_6O_4S$) : Calculated: C: 41.44, H: 1.93, N: 16.11; Found: C: 41.42, H: 1.87, N: 16.09.

3-azido-1-(4-(3-bromo-5-chloro-2-hydroxyphenyl)thiazol-2-yl)-4-(3-chlorophenyl) azetidin-2-one 3m

M.P.: 146 ^{0}C; IR (KBr): ν_{max}cm^{-1} 3492, 3133, 2086, 710, 667cm^{-1}; ^{1}H-NMR : δ 5.54-5.56 (d, 1H, *J* 9.52Hz, He), 5.92-5.93 (d, 1H, *J* 3.8Hz, Hf), 6.86-6.88 (d, 1H, *J* 6.52Hz, Hk), 7.11-7.46 (m, 4H, Hc,b,m,d), 7.68-7.70 (d, 1H, *J* 4.32Hz, Hl), 8.99 (s, 1H, Hg), 9.03 (s, 1H, Ar-OH); ^{13}C NMR : δ 59.5, 65.5, 99.2, 117.2, 125.2, 126.5, 127.8, 129.1, 130.0, 132.5, 135.5, 147.8, 149.8, 155.2, 160.7; MS (m/z) : (510.9M$^+$); Elemental Analysis ($C_{18}H_{10}BrCl_2N_5O_2S$) : Calculated: C: 42.29, H: 1.97, N: 13.70; Found: C: 42.27, H: 1.95, N: 13.67.

3-azido-1-(4-(3-bromo-5-chloro-2-hydroxyphenyl)thiazol-2-yl-4-(3-dimethylamino) phenyl) azetidin-2-one 3n

M.P.: >320 ^{0}C; IR (KBr): ν_{max}cm^{-1} 3450, 2987, 2109, 1680, 1510cm^{-1}; ^{1}H-NMR : δ 2.60 (s, 6H, Ar-N(CH_3)$_2$), 5.34-5.35 (d, 1H, *J* 1.84Hz, He), 5.91-5.92 (d, 1H, *J* 2.16Hz, Hf), 7.50 (s, 1H, Hg), 7.52-7.57 (d, 2H, *J* 20.7Hz, Ha,b), 7.59-7.67 (t, 1H), 7.74-7.77 (d, 1H, *J* 13.12Hz, Hk), 8.05-8.10 (q, 1H), 8.40 (s, 1H), 11.94 (s, 1H, Ar-OH); ^{13}C NMR : δ 40.2, 60.3, 65.1, 98.2, 114.1, 115.7, 124.2, 127.8, 129.6, 131.9, 133.0, 147.6, 153.0, 160.4; MS (m/z) : (519.99M$^+$); Elemental Analysis ($C_{20}H_{16}BrClN_6O_2S$) : Calculated: C: 46.21, H: 3.10, N: 16.17; Found: C: 46.19, H: 3.09, N: 16.15.

3-azido-1-(4-(5-chloro-2-hydroxyphenyl)thiazol-2-yl)-4-phenyl azetidin-2-one 3o

M.P.: 94 ^{0}C; IR (KBr): ν_{max}cm^{-1} 3452, 2088, 1740, 1650, 676cm^{-1} ; ^{1}H-NMR : δ 5.41-5.43 (d, 1H, *J* 8.6Hz, He), 5.88-5.89 (d, 1H, *J* 3.4Hz, Hf), 6.52 (s, 1H, Hg), 6.83-6.85 (d, 1H, *J* 9.04Hz, Hk), 7.12-7.38 (m, 6H, Ha,b,c,d,l,m), 7.65-7.67 (d, 1H, *J* 9.04Hz, Hi), 9.03 (s, 1H, Ar-OH); ^{13}C NMR : δ 60.2, 65.5, 101.7, 117.4, 123.8, 127.3, 129.8, 132.4, 144.5, 148.7, 154.3, 160.8; MS (m/z) : (397.04M$^+$); Elemental Analysis ($C_{18}H_{12}ClN_5O_2S$) : Calculated: C: 54.34, H: 3.04, N: 17.60 ; Found: C: 54.30, H: 3.02, N: 17.58.

3-azido-4-(furan-3-yl)-1-(4-(2-hydroxy-5-methyl-3-nitrophenyl) thiazol-2-yl) azetidin-2-one 3p

M.P.: 169 ^{0}C; IR (KBr): ν_{max}cm^{-1} 3466, 3109, 2110, 769, 682cm^{-1}; ^{1}H-NMR : δ 2.56 (s, 3H, Ar-CH_3), 6.17-6.19 (d, 1H, *J* 6.88Hz, He), 6.21-6.23 (d, 1H, *J* 6.88Hz, Hf), 6.21-6.23 (d, 1H, *J* 6.96Hz), 7.39-7.39 (d, 1H, *J* 2.32Hz), 7.50-7.53 (q, 1H), 7.67-7.69 (d, 1H, *J* 8.88Hz), 7.78-7.81 (m, 1H), 7.92-7.94 (d, 1H, *J* 9.04Hz), 9.23 (s, 1H, Ar-OH); ^{13}C NMR : δ 28.3, 43.3, 67.8, 100.2, 111.3, 123.8, 126.6, 129.8, 134.2, 138.6, 139.4, 139.9, 144.4, 149.8, 162.4; MS (m/z) : (412.0M$^+$); Elemental Analysis ($C_{17}H_{12}N_6O_5S$) : Calculated: C: 49.51, H: 2.93, N: 20.38; Found: C: 49.48, H: 2.91, N: 20.38.

3-azido-1-(4-(2-hydroxy-5methylphenyl)thiazol-2-yl)-4-phenyl azetidin-2-one 3q

M.P.: 184 ^{0}C; IR (KBr): ν_{max} cm^{-1} 3115, 2935, 2080, 1650, 1604, 750, 685cm^{-1}; ^{1}H-NMR : δ 1.59 (s, 3H, Ar-CH_3), 5.40-5.40 (d, 1H, *J* 3.16Hz, Hf), 5.69-5.70 (d, 1H, *J* 3.32Hz, He), 6.96-6.99 (d, 1H, *J* 8.88Hz, Hi), 7.44-7.49 (m, 5H, Ha,b,c,d,m), 7.57-7.58 (d, 1H, *J* 2.12Hz, Hi), 7.63 (s, 1H, Hg), 7.98 (s, 1H, Hk), 12.75 (s, 1H, Ar-OH); ^{13}C NMR : δ 24.6, 60.0, 65.5, 99.8, 116.3, 120.5, 126.8, 127.0, 127.6, 130.5, 131.5, 143.5, 148.5, 152.3, 160.4; MS (m/z) : (377.09M$^+$); Elemental Analysis ($C_{19}H_{15}N_5O_2S$) : Calculated: C: 60.46, H: 4.01, N: 18.56; Found: C: 60.46, H: 4.01, N: 18.55.

3-azido-1-(4-(5-chloro-2-hydroxy-3-iodophenyl)thiazol-2-yl)-4-(4-methoxyphenyl)azetidin-2-one 3r

M.P. : 145 ^{0}C; IR (KBr): ν_{max} cm^{-1} 3100, 2850, 2104, 1715, 690, 520cm^{-1}; ^{1}H-NMR : δ 3.68 (s, 3H, Ar-OCH_3), 5.81-5.84 (d, 1H, *J* 12.6Hz, He), 6.35-6.37 (d, 1H, *J* 6.68Hz, Hf), 7.44 (s, 1H, Hg), 7.50-7.52 (d, 1H, *J* 6.72Hz, Hl), 7.70-7.73 (d, 1H, *J* 4.00Hz, Hk), 7.86-7.88 (d, 2H, *J* 8.4Hz, Ha,b), 7.92-7.94 (d, 2H, *J* 9.08Hz, Hc,d), 9.17 (s, 1H, Ar-OH); ^{13}C NMR : δ 55.9, 62.0, 66.3, 89.4, 100.0, 114.1, 123.6, 127.8, 129.2, 130.8, 135.5, 139.2, 149.7, 158.7, 160.4,

163.2; MS (m/z) : (552.95M$^+$); Elemental Analysis ($C_{19}H_{13}ClN_5O_3S$) : Calculated: C: 41.21, H: 2.37, N: 12.65; Found: C: 41.19, H: 2.36, N: 12.64.

3-azido-1-(4-(5-chloro-2-hydroxy-3-iodophenyl)thiazol-2-yl)-4-(4-(dimethylamino)phenyl) azetidin-2-one 3s

M.P.: 132 ^{0}C; IR (KBr): ν_{max} cm^{-1} 3130, 2930, 2077, 1695, 665, 534cm^{-1}; ^{1}H-NMR : δ 2.80 (s, 6H, Ar-N(CH_3)$_2$), 5.49-5.50 (d, 1H, *J* 3.28Hz, He), 5.82-5.83 (d, 1H, *J* 3.44Hz, Hf), 6.55 (s, 1H, Hg), 6.66-6.70 (d, 2H, *J* 16.2Hz, Ha,b), 7.15-7.17 (d, 2H, *J* 8.52Hz, Hc,d), 7.36-7.38 (d, 1H, *J* 6.84Hz, Hl), 7.66-7.68 (d, 1H, *J* 8.08Hz, Hk), 8.82 (s, 1H, Ar-OH); ^{13}C NMR : δ 40.3, 59.8, 64.3, 89.7, 101.2, 116.3, 121.7, 126.6, 128.6, 130.7, 133.3, 140.5, 147.6, 148.2, 162.2, 164.8; MS (m/z) : (565.98M$^+$); Elemental Analysis ($C_{20}H_{16}ClN_6O_2S$) : Calculated: C: 42.38, H: 2.85, N: 14.83; Found: C: 42.37, H: 2.84, N: 14.81.

Biological assay

The minimum inhibitory concentration (MIC) exercises completed in 50, 100, 200μg/ml DMSO by a disc-plate method utilizing the nutrient agar mediums. Gentamycin, doxycycline, and fluconazole used as standards, the minimum inhibitory concentration for the most dynamic strategies (Chang et al., 1997). Filter paper disc method (Vincent & Vincent, 1944) using the Hi-Media agar mediums is employed to study the antibacterial activity of **3a-s** against Gram-positive bacteria Staphylococcus aureus, Gram-negative bacteria Pseudomonas aeruginosa and Escher-

ichia coli bacterial strain and Candida Albicans as antifungal strain. Preparation of nutrient broth, subculture, and base layer medium has done as per the standard procedure. Each test compound (40mg) dissolved in 2mL of DMSO, which used as a sample solution. Different concentrations (200, 100, 50µg/mL) of the solution prepared by the dilution method. The sample size for all the compounds fixed as 10µL. The paper disc of each test compound placed on the previously inoculated petri dish with the microorganisms. After 24hr and 48hr treatment for antibacterial and antifungal study, a zone of inhibition produced by each compound measured in mm.

Computational details

All the ligand used was made using ChemDraw 3D (ultra-Software., n.d.). Before the docking calculation of the ligands, the structure was lower in energy and then docked by using PyRx (Trott & Olson, 2010). The crystal structure for the complex with an inhibitor downloaded from Protein Data Bank (http://www.rscb.org/) as a PDB file. The active site of the docked protein was found out by Argus Lab 4.0 (software., n.d.), which used for the docking in the PyRX.

The downloaded protein of the PBP2a clinical mutant E150K from MRSA (PDB ID- 4BL2) contain chain A and B with chloride and cadmium ion as an interacting ligand. The protein contains two chains A, and B has 20519 atoms with net charge is zero and having 57051 valence electrons. The protein-ligand interaction studied with the active binding site of chains A and B. In the chain A contains nineteen active binding sites viz. ALA301, ARG110, ARG298, ASN307, ASP209, GLN137, GLN140, GLN207, GLU145, GLY135, HIS143, HIS232, HIS311, ILE309, LYS229, LYS230, THR210, THR300 and VAL302 in chain B contain twenty-one active binding site that is VLA952, ARG752, ASN949, ASN1211, ASP851, ASP1215, GLN779, GLN782, GLN849, GLU787, GLY777, HIS785, HIS874, HIS953, ILE786, ILE943, ILE951, LYS1093, MET778, THR942, and VAL944. The chain A and B with the residues, water, and hetero group within a radius of $2.72A^0$ refined for further cleaned by ascertaining the hybridization and introducing the H-atoms to the protein residue with the removal of water molecules. The docking with PyRx (Autodock) was conducted vina search space of dimension size x = 55.4589539785, y = 37.7989937242, z = 43.9275995514, center x = 22.7466396916, y = 37.934731349, z = 23.0487215997 for chain A and for chain B size x = 69.314661892, y = 33.6138645394, z = 90.4083639469, x = 1.67346816513, y = 38.8272936698, z = 45.4518205308 with eight exhaustiveness. The LIGPLO T+ version V.1.4.5 (Laskowski & Swindells, 2011) used to find the multiple ligand-protein interaction diagram.

SIB site http://www.swissadme.ch retrieved to in an internet browser that shows the lodging page of SwissADME. Our synthesized and categorized molecules **3a-s** and standard drug were a contribution for estimation of ADME, physicochemistry,

drug-likeness similarity, pharmacokinetics, and therapeutic properties. The effort zones itself include a molecular sketcher dependent on ChemAxon's Marvin JS (http://www.chemaxon.com) that enabled the client to draw and alter 2D chemical structures. The structures moved as a rundown to the right-hand side of the lodging page, which is the real contribution for computational calculation. The list made to contain one input molecule for each line, characterized by the simplified molecular-input line-entry system (SMILES), and results are introduced for every molecule in tables, graphically, and as an excel spreadsheet.

Acknowledgments. Authors are thankful to the Department of Pharmacy, Nagpur for IR spectral analysis, and SAIF, Chandigarh, for ^{1}H NMR spectral analysis. We are grateful to SAIF, Pune University, for mass spectral analysis of all newly synthesized compounds. We pay special thanks to Dr. Mrs. Sandhya Saoji for antimicrobial activity.

REFERENCES

Akiyama, T., Takaya, J. & Kagoshima, H. (1999). Brønsted acid-catalyzed aza Diels-Alder reaction of Danishefsky's diene with aldimine generated in situ from aldehyde and amine in aqueous media. *Tetrahedron Lett., 40*, 7831 – 7834.

Amantini, D., Fringuelli, F., Pizzo, F. & Vaccaro, L. (2002). Selected methods for the reduction of the azido group. *Org. Prepar. & Proced. Int., 34*, 109 – 147.

Beck, W. & Fehlhammer, W.P. (1967). Ligand addition and redox reactions of azido-metal complex. *Angew. Chem. Int. Ed. Engl., 6*, 169 – 170.

Bose, A.K., Manhas, M.S., Van der Veen, J.M, Bari, S.S. & Wagle, D.R. (1992). Stereoregulated synthesis of β-lactams from schiff bases derived from threonine esters. *Tetrahedron, 48*, 4831 – 4844.

Botta, O., Moyroud, E., Lobato, C. & Strazewsky, P. (1998). Synthesis of 3′-azido- and 3′-amino-3′-deoxyadenosine in both enantiomeric forms. *Tetrahedron, 54*, 13529 – 13546.

Brenk, R., Schipani, A., James, D., Krasowski, A., Gilbert, I.H., Frearson, J. & Wyatt, P.G. (2008). Lessons learnt from assembling screening libraries for drug discovery for neglected diseases. *Chem. Med. Chem., 3*, 435 – 444.

Busetto, L., Pallazzi, A. & Ros, R. (1975). Preparation and reactivity of some new azido-bridged complexes of Pd(II) and Pt(II). *Inorg. Chim. Acta, 13*, 233 – 238.

Cardillo, G., Fabbroni, S., Gentilucci, L., Perciaccante, R., Piccinelli, F. & Tolomelli, A. (2005). Highly diastereoselective allylic azide formation and isomerization. synthesis of 3(2'-amino)-β-lactams. *Org. Lett., 7*, 533 – 536.

Chang, J.-C., Hsueh, P.-R., Wu, J.-J., Ho, S.-W,, Hsieh, W-C. & Luh, K-T. (1997). Antimicrobial susceptibility of flavobacteria as determined by agar dilution and disk diffusion methods. *Antimicrobial Agents & Chemotherapy, 41*, 1301 – 1306.

Daina, A. & Zoete, V. (2016). A BOILED-Egg to predict gastrointestinal absorption and brain penetration of small molecules. *Chem. Med. Chem., 11*, 1117 – 1121.

Daina, A., Michielin, O. & Zoete, V. (2017). SwissADME: a free web tool to evaluate pharmacokinetics, drug-likeness and medicinal chemistry friendliness of small molecules. *Sci Rep., 7*, art. no. 42717.

Daum, R.S., Ito, T., Hiramatsu, K., Hussain, F., Mongkolrattanothai, K., Jamklang, M. & Boyle-Vavra, S. (2002). A novel methicillin-resistance cassette in community-acquired methicillin-resistant staphylococcus aureus isolates of diverse genetic backgrounds. *J. Infectious Diseases, 186*, 1344 – 1347.

Delaney, J.S. (2004). Esol: estimating aqueous solubility directly from molecular structure. *J. Chem. Inf. Comput. Sci., 44*, 1000 – 1005.

Demeshkina, N.A., Laletina, E.S., Meschaninova, M.I., Repkova, M.N., Venyaminova, A.G., Graifer, D.M. & Karpova, G.G. (2003a). The mRNA codon environment at the P and E sites of human ribosomes deduced from photocrosslinking with pUUUGUU derivatives. *Mol. Biol., 37*, 132 – 139.

Demeshkina, N.A., Laletina, E.S., Meschaninova, M.I., Venyaminova, A.G., Graifer, D.M. & Karpova, G.G. (2003b). Positioning of mRNA codons with respect to 18S rRNA at the P and E sites of human ribosome. *Biochim. Biophys. Acta., 1627*, 39 – 46.

Dezhurov, S.V., Khodyreva, S.N., Plekhaniva, E.S. & Lavrik, O.I. (2005). A new highly efficient photoreactive analogue of dCTP: synthesis, characterization, and application in photoaffinity modification of DNA binding proteins. *Bioconjugate Chem., 16*, 215 – 222.

Egan, W.J., Merz, K.M. & Baldwin, J.J. (2000). Prediction of drug absorption using multivariate statistics. *J. Med. Chem., 43*, 3867 – 3877.

El Akri, K., Bougrin, K.., Balzarini, J., Faraj, A. & Benhida, R. (2007). Efficient synthesis and in vitro cytostatic activity of 4-substituted triazolylnucleosides. *Bioorg. & Med. Chem. Lett., 17*, 6656 – 6659.

Fagerberg, J.H., Karlsson, E., Ulander, J., Hanisch, G. & Bergström, C.A.S. (2015). Computational prediction of drug solubility in fasted simulated and aspirated human intestinal fluid. *Pharm. Res., 32*, 578 – 589.

Feldman, A.K., Colasson, B., Sharpless, K.B. & Fokin, V.V. (2005). The allylic azide rearrangement: achieving selectivity. *J. Amer. Chem. Soc., 127*, 13444 – 13445.

Fehlhammer, W.P., Kemmerich, T. & Beck, W. (1979). Reaktionen von azidocobalt(III)-chelatkomplexen mit isocyaniden.*Chem. Ber., 112*, 468 – 479.

Fishovitz, J., Rojas-Altuve, A., Otero, L.H., Dawley, M., Carrasco-López, C., Chang, M., Hermoso, J.A. & Mobashery, S. (2014). Disruption of allosteric response as an unprecedented mechanism of resistance to antibiotics. *J. Amer. Chem. Soc., 136*, 9814 – 9817.

Ghatole, A.M., Lanjewar, K.R, & Gaidhane, M.K. (2012). Syntheses, characterization, antimicrobial activity of copper (II), zinc (II) and cobalt (II) complexes of the bi-dented substituted 2-((E)-2-((2-chloro-6-ethoxyquinolin-3-yl). *J. Pharm. Res., 5*, 2758 – 2762.

Ghatole, A.M., Lanjewar, K.R. & Gaidhane, M.K. (2014). Synthesis and anti-microbial activity of some substituted bis[2-((E)-2-(4-benzylideneamino)thiazol-4-Yl)-4-methylphenol] metal complexes. *Int. J. Pharmacy & Pharmaceutical Sci., 6*, 142 – 146.

Ghatole, A.M., Lanjewar, K.R., Gaidhane, M.K. & Hatzade, K.M. (2015). Evaluation of substituted methyl cyclohexanone hybrids for anti-tubercular, anti-bacterial and anti-fungal activity: facile syntheses under catalysis by ionic liquids. *Spectrochimica Acta Part A: Molecular & Biomolecular Spectroscopy, 151*, 515 – 524.

Ghose, A.K., Viswanadhan, V.N. & Wendoloski, J.J. (1999). A knowledge-based approach in designing combinatorial or medicinal chemistry libraries for drug discovery. 1. A qualitative and quantitative characterization of known drug databases. *J. Comb. Chem., 1*(1), 55 – 68.

Gordon, C.M. (2001). New developments in catalysis using ionic liquids. *Appl. Catalysis A: Gen., 222*, 101 – 117.

Hakimelahi, G.H. & Sardarian, A.R. (1990). Synthesis of derivatives of (1R*,10aR*)-1-azido-10-benzylidene-4-(diethylphosphono)-1,2,10,10a-tetrahydro-2-oxo-4H-azeto[1,2-a]pyrido[1,2-d]pyrazin-9-ylium bromide. *Helvetica Chem. Acta, 73*, 180 – 184.

Han, S.-Y, Choi, S.H., Kim, M.H., Lee, W.G., Kim, S.H., Min. Y.K. & Kim, B.T. (2006a). Design and synthesis of novel photoaffinity reagents for labeling VEGF receptor tyrosine kinases. *Tetrahedron Lett., 47*, 2915 – 2919.

Han, S.-Y., Park, S.-S., Lee, W.G., Min, Y.K. & Kim, B.T. (2006b). Synthesis of a novel biotin-tagged photoaffinity probe for VEGF receptor tyrosine kinases. *Bioorg. & Med. Chem. Lett., 26*, 129 – 133.

Katritzky, A.E., Qiu, G., He, H.-Y. & Yang, B. (2000). Novel syntheses of hexahydro-1H-pyrrolo[1,2-a]imidazoles and octahydroimidazo[1,2-a] pyridines. *J. Org. Chem., 65*, 3683 – 3689.

Larock, R.C. (1989). *Comprehensive organic transformations: a guide to functional group preparations.* New York: VCH.

Laskowski, R.A. & Swindells, M.B. (2011). LigPlot+: multiple ligand-protein interaction diagram for drug discovery. *J. Chem. Inf. Model., 51*, 2778 – 2786.

Lavrik, O.I., Prasad, R., Beard, W.A., Safronov, I.V., Dobrikow, M.I., Wood, T.G. & Wilson, S.H. (1996). dNTP binding to HIV-1 reverse transcriptase and mammalian DNA polymerase β as revealed by affinity labeling with a photoreactive dNTP analog. *J. Biol. Chem., 271*, 21891 – 21897.

Lee, B.-in, Nguyen, L.H., Barsky, D., Fernandes, M. & Wilson rd, D.M. (2002). Molecular interactions of human Exo1 with DNA. *Nucleic Acids Res., 30*, 942 – 949.

Lin, J., Wang, M., Hu, H., Yang, X., Wen, B., Wang, Z., Jacobson, O., Song, G., Huang, P. & Chen, X. (2016). Multimodal-imaging-guided cancer phototherapy by versatile biomimetic theranostics with UV and γ-irradiation protection. *Adv. Mater., 28*, 3273 – 3279.

Lipinski, C.A., Lombardo, F., Dominy, B.W. & Feeney, P.J. (2001). Experimental and computational approaches to estimate solubility and permeability in drug discovery and development settings. *Adv Drug Deliv Rev., 46*, 3 – 26.

Mangelinckx, S., Boeykens, M., Vliegen, M., Van der Euken, K. & De Kimpe, N. (2005). Symthesis of new 3,3-dimethoxyazetidine-2-carboxylic acid derivatives. *Tetrahedron Lett., 46*, 525 – 529.

Mitchell, D.A., Jones, N.A., Hunter, S.J., Cook, J.M.D., Jankinson, S.F., Wormald, M.R., Owek, R.A. & Fleet, G.W.J. (2007). Symthesis of 2-C-branced derivatives of D-mannose: 2-C-aminomethyl-D-mannose binds to the human S-type lectin DC-SIGN with affinity greater than an order of magnitude compared to that of D-mannose. *Tetrahedron: Asymmetry, 18*, 1502 – 1510.

Muegge, I., Heald, S.L. & Brittelli, D. (2001). Simple selection criteria for drug-like chemical matter. *J. Med. Chem., 44*, 1841 – 1846.

Nyffeler, P., Liang, C., Koeller, K. & Wong, C. (2002). The chemistry of amine-azide interconversion: catalytic diazotransfer and regioselective azide reduction. *J. Amer. Chem. Soc., 124*, 10773 – 10778.

Ogu, C.C.. & Maxa, J.L. (2000). Drug interaction due to cytochrome P450. *Proc (Bayl Univ Med Cent)., 13*, 421 – 423.

Pino-González, M.-S., Assiego, C. & Ona, N. (2008). Studies on reactivity of azidoamides, intermediates in the synthesis of tetrahydroxypipecolic acid derivatives. *Tetrahedron Asymmetry, 19*, 932 – 937.

Rigby, W., Bailey, P.M., McCleverty, J.A. & Maitlis, P.M. (1979). Crystal and molecular structures of pentane-2,4-dionato-(α, 1,2-η-triphenylmethyl)-palladium and -platinum. *J. Chem. Soc., Dalton Trans.*, 346 – 350.

Rossi, F., Diaz, L., Wollam, A., Panesso, D., Zhou, Y., Rincon, S., Narechania, A., Xing, G., Thias, S.R., Di Gioia, M.D., Doi, A., Tran, T.T., Reyes,

J., Munita, J.M., Carvajal, L.P., Hernandez-Roldan, A., Brandao, D., Van der Heijden, I.M., Murray, B.E., Planet, P.J., Weinstock, G.M. & Arias, C.A. (2014). Transferable vancomycin resistance in a community-associated MRSA lineage. *New England J. Med., 370*, 1524 – 1531.

Rostovtsev, V., Green, L., Fokin, V. & Sharpless, K. (2002). A sepwise huisgen cycloaddition process: copper(I) catalyzed regioselective "ligation" of azides and terminal alkynes. *Angew. Chem. Int. Ed., 41*, 2596 – 2599.

Schnapp, K.A, Poe, R., Leyva, E., Soundararajan, N. & Platz, M.S. (1993). Exploratory photochemistry of fluorinated aryl azides. Implications for the design of photoaffinity labeling reagents. *Bioconjugate Chem., 4*, 172 – 177.

Scriven, E. & Turnbull, K. (1988). Azides: their preparation and synthetic uses. *Chem. Rev., 88*, 297 – 368.

Sheldon, R. (2001). Catalytic reactions in ionic liquids. *Chem.l Commn.*, No. 23, 2399 – 2407.

Silverman, R.B. & Dolphin, D.J. (1976). Model studies for coenzyme B12 dependent enzyme-catalyzed rearrangements: evidence for cobalt(III)-olefin .pi. complexes. *J. Amer. Chem. Soc., 98*, 4626 – 4633.

Trott, O. & Olson, A.J. (2010). AutoDock Vina: improving the speed and accuracy of docking with a new scoring function, efficient optimization, and multithreading. *J. Comp. Chem., 31*, 455 – 461.

Veber, D.F., Johnson, S.R., Cheng, H.-Y., Smith, B.R.,Ward, K.W. & Kopple, K.D. (2002). Molecular properties that influence the oral bioavailability of drug candidates. *J. Med. Chem., 45*, 2615 – 2623.

Vincent, J.G. & Vincent, H.M. (1944). Filter paper disc modification of the Oxford cup penicillin determination. *Proc. Soc. Exp. Biol. & Med., 55*(3), 162 – 164.

Wenzel, A.G. & Jacobsen, E.N. (2002). Asymmetric catalytic Mannich reactions catalyzed by urea derivatives: enantioselective synthesis of β-aryl-β-amino acids. *J. Amer. Chem. Soc., 124*, 12964 – 12965.

Zarei, M. & Jarrahpour, A. (2011). A mild and efficient route to 2-azetidinones using the cyanuric chloride-DMF complex. *Synlett., 17*, 2572 – 2576.

✉ **Dr. A. M. Ghatole (corresponding author)**
Dhote Bandhu Science College
Gondia, 441614, India
E-mail: ajay.ghatole5@gmail.com
kishorhatzade@gmail.com.